Published in final edited form as:
J Comp Neurol. 2006 July 1; 497(1): 42–60. doi:10.1002/cne.20972.

Developmental Regulation of α-Amino-3-Hydroxy-5-Methyl-4-Isoxazole-Propionic Acid Receptor Subunit Expression in Forebrain and Relationship to Regional Susceptibility to Hypoxic/Ischemic Injury. I. Rodent Cerebral White Matter and Cortex

Delia M. Talos[1,2], **Rachel E. Fishman**[1], **Hyunkyung Park**[1,2], **Rebecca D. Folkerth**[2,3,4], **Pamela L. Follett**[1,2], **Joseph J. Volpe**[1,2,5], and **Frances E. Jensen**[1,2,5,*]

[1]Department of Neurology, Children's Hospital, Boston, Massachusetts 02115

[2]Harvard Medical School, Boston, Massachusetts 02115

[3]Department of Pathology (Neuropathology), Children's Hospital, Boston, Massachusetts 02115

[4]Department of Pathology, Brigham and Women's Hospital, Boston, Massachusetts 02115

[5]Program in Neuroscience, Harvard Medical School, Boston, Massachusetts 02115

Abstract

This is the first part of a two-part study to investigate the cellular distribution and temporal regulation of α-amino-3-hydroxy-5-methyl-4-isoxazole-propionic acid receptor (AMPAR) subunits in the developing white matter and cortex in rat (part I) and human (part II). Western blot and immunocytochemistry were used to evaluate the differential expression of AMPAR subunits on glial and neuronal subtypes during the first 3 postnatal weeks in the Long Evans and Sprague Dawley rat strains. In Long Evans rats during the first postnatal week, GluR2-lacking AMPARs were expressed predominantly on white matter cells, including radial glia, premyelinating oligodendrocytes, and subplate neurons, whereas, during the second postnatal week, these AMPARs were highly expressed on cortical neurons, coincident with decreased expression on white matter cells. Immunocytochemical analysis revealed that cell-specific developmental changes in AMPAR expression occurred 2–3 days earlier by chronological age in Sprague Dawley rats compared with Long Evans rats, despite overall similar temporal sequencing. In both white and gray matter, the periods of high GluR2 deficiency correspond to those of regional susceptibility to hypoxic/ischemic injury in each of the two rat strains, supporting prior studies suggesting a critical role for Ca^{2+}-permeable AMPARs in excitotoxic cellular injury and epileptogenesis. The developmental regulation of these receptor subunits strongly suggests that Ca^{2+} influx through GluR2-lacking AMPARs may play an important role in neuronal and glial development and injury in the immature brain. Moreover, as demonstrated in part II, there are

*Correspondence to: Frances E. Jensen, Enders 348, Department of Neurology, Children's Hospital, 300 Longwood Avenue, Boston, MA 02115. frances.jensen@childrens.harvard.edu.

striking similarities between rat and human in the regional and temporal maturational regulation of neuronal and glial AMPAR expression.

Indexing terms

glutamate receptor; perinatal; excitotoxicity; seizure; neuron; oligodendrocyte

The immature brain is highly susceptible to hypoxia/ischemia (H/I), and perinatal H/I brain injury represents a major cause of neurodevelopmental disorders in both preterm and term infants (Volpe, 2001; Ferriero, 2004). In preterm infants, H/I causes primarily white matter injury, termed *periventricular leukomalacia* (PVL; Banker and Larroche, 1962; Okumura et al., 1997; Volpe, 2001). In contrast, H/I in term newborns causes predominantly gray matter lesions and seizures (Hauser et al., 1993; Maller et al., 1998; Roland et al., 1998; Saliba et al., 1999; Volpe, 2001).

Rodent models of perinatal H/I brain injury reflect similar age-dependent regional differences, despite slight age variations in different rat strains. During the first week of life (postnatal day P1–P7), H/I results in selective white matter injury, characterized by loss of premyelinating oligodendrocytes (pre-OLs), followed by hypomyelination (Sheldon et al., 1996; Follett et al., 2000; Cai et al., 2001; Back et al., 2002; Liu et al., 2002). During the second postnatal week (P8–14), H/I causes spontaneous electro-graphic and behavioral seizures (Jensen et al., 1991; Owens et al., 1997), as well as extensive cortical and hippocampal neuronal loss (Towfighi et al., 1997; Chen et al., 1998).

H/I causes glutamate accumulation in both gray and white matter structures in the developing rat brain (Benveniste et al., 1984; Andine et al., 1991; Silverstein et al., 1991; Hagberg, 1992; Loeliger et al., 2003), implying a key role for glutamate receptors (GluRs) in the pathophysiology of perinatal H/I brain injury. Glutamate receptor subtypes include the N-methyl-D-aspartate receptors (NMDARs), the α-amino-3-hydroxy-5-methyl-4-isoxazole-propionic acid receptors (AMPARs), and kainate receptors (KARs; Hollmann and Heinemann, 1994; Michaelis, 1998). Whereas neurons and astrocytes express both NMDARs and non-NMDARs (Petralia and Wenthold, 1992; Petralia et al., 1994; Conti et al., 1994; Shelton and McCarthy, 1999; Schipke et al., 2001), OLs express primarily non-NMDARs (Patneau et al., 1994; Gallo et al., 1994; Rosenberg et al., 2003). Compelling evidence for a critical role of GluRs in perinatal H/I injury is provided by experimental therapeutic trials. AMPAR antagonists are highly protective to developing OLs against H/I injury at P7 (Follett et al., 2000, 2004) and are effective in suppressing hypoxia-induced seizures at P10–P12 (Jensen et al., 1995; Koh and Jensen, 2001). Similarly, in P7–P10 rats, NMDAR and AMPAR antagonists have been shown to attenuate H/I-induced neuronal injury (Olney et al., 1989; Hagberg et al., 1994; Chen et al., 1998).

AMPAR-mediated signaling and excitotoxicity depend on the functional properties of the receptor complex, such as Ca^{2+} permeability (Gu et al., 1996; Friedman and Koudinov, 1999; Sanchez et al., 2001, 2005; Jensen et al., 2001; Deng et al., 2003; Follett et al., 2004), which in turn are dictated by subunit composition. AMPARs are heteromeric complexes composed of four subunits (GluR1 through GluR4), and receptors lacking the GluR2 subunit

are Ca^{2+}-permeable, whereas those including the GluR2 subunit are impermeable to Ca^{2+} (Burnashev et al., 1992; Seeburg, 1993; Jonas et al., 1994; Washburn et al., 1997). In the immature rat brain, GluR2 expression is low relative to non-GluR2 subunits (Pellegrini-Giampietro et al., 1991, 1992; Sanchez et al., 2001; Kumar et al., 2002), suggesting that AMPARs with increased Ca^{2+} permeability are abundantly expressed during this time window. Indeed, functional studies in situ in immature rodent brain have confirmed increased Ca^{2+} influx through AMPARs expressed on pre-OLs (Fulton et al., 1992; Bergles et al., 2000; Follett et al., 2004) and developing hippocampal and pyramidal neurons (Sanchez et al., 2001; Kumar et al., 2002), supporting a close correlation between GluR2 expression level and receptor function.

In this two-part series of studies, we examine evidence for a relationship between differential distribution of GluR2-lacking (Ca^{2+}-permeable) AMPARs and selective white and gray matter vulnerability to H/I in both rodent (part I) and human (Talos et al., 2006). We hypothesize that the GluR2-lacking AMPARs represent a key factor in age-dependent regional susceptibility to H/I, so regional and temporal expression of these receptors would correspond in a cell-specific manner to patterns of susceptibility to H/I. In addition, we hypothesize that subtle differences in age windows of susceptibility between rat strains are due to strain-dependent differences in temporal onset and progression of AMPAR subunits on specific cell types. In part I, we analyzed the developmental profile of each AMPAR subunit in both white matter and cortex from Long Evans (LE) rats during the first 3 postnatal weeks (postnatal days P1–P21) and specifically evaluated the developmental regulation of the GluR2 subunit relative to other AMPAR subunits by immunoblotting and immunofluorescence double labeling. To examine strain-dependent differences in AMPAR subunit expression, a subset of immunofluorescence double-labeling experiments for specific AMPAR subunits was conducted in parallel in both LE and Sprague Dawley (SD) rat pups, ages P1–P14. In part II (Talos et al., 2006), human parietal white matter and cortex from cases ranging between 18 postconceptional weeks (PCW) and 210 PCW (approximately 3.3 years) were similarly evaluated for age-dependent variations in AMPAR subunit expression by immunoblotting and immunofluorescence double labeling.

MATERIALS AND METHODS

Animals

Long Evans and Sprague Dawley rats (Charles River Laboratories, Wilmington, MA) were housed in a temperature-controlled animal care facility with a 12-hr light/dark cycle. All procedures were approved by and in accordance with the guidelines of the Animal Care and Use Committee at Children's Hospital (Boston, MA) and the National Institutes of Health Guide for the Care and Use of Laboratory Animals. All efforts were made to minimize animal suffering and the number of animals used.

Western blot analysis

Immunoblotting—LE rats were sacrificed at P3, P5, P7, P9, P11, P14, and P21 and at adulthood (n = 30). Brains were quickly removed, and either cortex or white matter samples were separated under a dissecting microscope. Tissue was rapidly frozen in ethanol and

stored at −80°C until it was used for protein extraction. Membrane protein extraction was conducted according to the protocol described by Wenthold et al. (1992). Dissected cortex and white matter samples were homogenized separately in a sucrose buffer (11% sucrose, 500 nM $CaCl_2$, 1 μM $MgCl_2$, 1 μM $NaHCO_3$) containing one Complete Mini, ethyl-enediaminetetraacetic acid (EDTA)-free protease inhibitor cocktail tablet (Roche, Indianapolis, IN) per 10 ml of buffer. Membrane fractions were collected and resus-pended in lysis buffer: 50 mM trizma base, 1% igepal CA-630, 150 mM NaCl, 0.1% leupeptin, 1 mM benzami-dine, 1 mM EDTA, 1 mM phenylmethylsulfonyl fluoride (PMSF). Total protein amounts were measured by using the Bradford protein assay (Bio-Rad, Hercules, CA), and samples were diluted for equal amounts of protein in each sample. Samples were run on 7.5% Tris-HCl gels (Bio-Rad) and transferred onto polyvinylidene difluoride (PVDF) membranes. A Coomassie blue stain (Sigma, St. Louis, MO) was performed on each gel to verify the consistency of protein loading across lanes. Membranes were blocked for 1 hour in 5% nonfat dry milk in Tris-buffered saline with 0.1% Tween 20 and incubated overnight at 4°C in primary antibodies (Table 1). Blots were then incubated for 1 hour at room temperature (RT) in horseradish peroxidase-conjugated secondary antibodies: anti-mouse IgG (0.5 μg/ml; Jackson Immunoresearch Laboratories, West Grove, PA) or anti-rabbit IgG (0.1 μg/ml; Jackson Immunoresearch Laboratories). Protein bands were visualized by using Western Lightning chemiluminescence reagent (Perkin Elmer, Wellesley, MA) and developed on X-ray film (X-Omat AR; Kodak, Rochester, NY). The blots were stripped (Renart and Sandoval, 1984) and reprobed with antibodies against different AMPAR subunits. Protein dilution series were performed to assess whether all optical densities fell within a linear range.

Data analysis—The films were scanned, and band intensities were converted to relative optical signal density by subtracting the background optical density from each band in Quantity One software (Bio-Rad). In each case, the relative optical density was normalized to the mean level of expression of the same adult samples run on each blot. Means for each age group were calculated for each antibody (a minimum of three animals/age group) and were compared across ages via one-way ANOVA and post hoc *t*-tests. Differences were considered significant at $P < 0.05$. To determine the relative levels of expression of GluR2 to non-GluR2 subunits, GluR1/GluR2, GluR3/GluR2, GluR4/GluR2, and total non-GluR2 (GluR1 + GluR3 + GluR4)/GluR2 ratios were also calculated in each case, by using the normalized individual GluR1–GluR4 values (percentage of adult). The group means were similarly compared across development, and differences were considered significant at $P < 0.05$ (one-way ANOVA and post hoc *t*-tests).

Immunocytochemistry

Immunostaining of tissue sections—LE rat pups ages P1, P3, P5, P7, P9, P10, P11 P14, P18, and P21 (n = 46) and SD pups ages P1, P3, P5, P7, P10, and P14 (n = 30) were deeply anesthetized (pentobarbital i.p. 50–100 mg/kg, depending on postnatal age) and perfused intracardially with 0.1 M phosphate-buffer saline (PBS), followed by 4% paraformaldehyde in PBS (pH 7.4). Brains were subsequently removed, postfixed for 4 hours in the same paraformaldehyde-containing solution, and cryoprotected in 30% sucrose overnight. Coronal sections, cut at 50 μm on a freezing microtome (HM 440 E; Microm

International), were collected serially and maintained in 0.1% sodium azide in PBS at 4°C until use. To block nonspecific binding, sections were first incubated for 1 hour at room temperature in a solution containing 0.1% Triton X-100 and 5% normal goat serum in PBS (Invitrogen, Carlsbad, CA), except for those to be stained with oligodendroglial markers O4, GalC, and O1, when 0.1% Triton X-100 was omitted. Sections were then exposed to the primary antibodies overnight at 4°C (Table 1). After three 10-minute PBS washes, sections were incubated with the secondary antibodies. For GluR1–GluR4 immunocytochemistry, sections were incubated for 1 hour at RT with a biotinylated anti-rabbit/anti-mouse IgG (1:200; Vector Laboratories, Burlingame, CA), washed for 3 × 10 minutes in PBS, followed by 1 hour incubation at RT with a fluoresceinavidin D conjugate (1:2,000; Vector Laboratories). For the other antibodies, slides were incubated for 1 hour at RT with a secondary antibody solution containing Alexa Fluor 568 goat anti-rabbit/anti-mouse IgG/IgM or Oregon green 488 goat anti-rabbit/anti-mouse IgG (1:1,000; Molecular Probes, Eugene, OR). After secondary antibody incubation, sections were washed for 3 × 10 minutes in PBS and coverslipped with an antifade medium (Fluoromount-G; Southern Biotechnology, Birmingham, AL). Monoclonal astroglial markers vimentin and glial fibrillary acidic protein (GFAP), oligodendroglial markers O4, O1, and MBP, and neuronal markers NeuN and GAD-65 were used in combination with polyclonal antibodies GluR1, GluR2, and GluR4. Polyclonal cell markers GFAP, GalC, NSE, and GABA were used in combination with monoclonal GluR3 antibodies. In each double-labeling experiment, control sections were incubated with omission of one or both primary antibodies, adding only the secondary antibodies to exclude false-positive labeling.

Data analysis—Slides were analyzed with an epifluorescence microscope (Zeiss Axioscope, Germany). Data was obtained by examining a minimum of three brains/age group/staining condition, and the expression pattern for each antibody was analyzed on at least three sections/brain. Developmental regulation of AMPAR expression, including cell-type-specific subunit characteristics, timing of presentation, expression level, regional distribution pattern, and subcellular localization, was qualitatively analyzed. Relative staining intensity for each subunit was compared in one cell type across ages and between cell populations in white matter and cortex at a specific age. In all cases, sections to be analyzed were processed together to permit such comparisons.

Preparation of illustrations—Digital images of the immunostained tissue sections were acquired with a Spot digital camera in the Spot Software 4.5 (Diagnostic Instruments, Sterling Heights, MI). Original digitized RGB images were transferred to Adobe Photoshop 7.0 (Adobe Systems, San Jose, CA), and the brightness, contrast and color were adjusted to achieve optimal quality of the resulting prints. These minimal adjustments did not alter in any way the immunofluorescence staining pattern of the antibodies.

Antibodies

AMPAR subunit-specific antibodies and cell-specific markers used in this study have been characterized extensively in a variety of species and brain regions, including rat forebrain. Primary antibody characterization is summarized in Table 1, and previous studies demonstrating the antibody specificity are listed at the bottom of the table. Additionally,

GluR1–GluR4 antibody specificity in tissue homogenates was demonstrated by the presence of single bands on both white matter and cortex Western blots, corresponding to the molecular weight specified by vendor, and in tissue sections by a staining pattern consistent with previous reports (Wenthold et al., 1992; Petralia et al., 1997; Sanchez et al., 2001; Kumar et al., 2002; Grunert et al., 2003; Moga et al., 2003; Lindahl and Keifer, 2004). The specificity of anti-GluR1 and anti-GluR4 antibodies was further verified by preabsorption with the corresponding immunogenic peptides. In Western blotting, peptide preabsorption (10:1–20:1 antigen:antibody concentration; Chemicon International, Temecula, CA) completely eliminated GluR1 and GluR4 bands and in tissue sections, peptide preabsorption of the GluR1 and GluR4 antiserum (10:1 antigen:antibody concentration; Chemicon International) blocked all immunostaining with the antibodies.

All cell markers used in this study produced a staining pattern comparable to patterns in previous studies using the same antibodies. Vimentin labeled the radial glia cell bodies and processes, whereas GFAP antibodies stained both radial glia and mature astrocytes (Miyata et al., 2001; Zhou et al., 2004). The staining pattern of polyclonal GFAP antiserum largely overlapped with that of monoclonal GFAP; however, radial glia was stained more effectively with the polyclonal than with the monoclonal GFAP antibody. The O1 and O4 monoclonal antibodies are known to react specifically with surface antigens expressed on developing oligodendrocytes in a stage-specific manner. O1 recognizes the GalC and the closely related monogalactosyl-digliceride (MG) expressed on the surface of immature OLs, whereas O4 antibody reacts with two related sulfated galactolipids (sulfatide and seminolipid), expressed on OL precursor cell surface, prior to O1 (Gard and Pfeiffer, 1989). In this study, both antibodies stained cell bodies and processes of developing OLs, whereas the MBP antibody labeled mature OLs, as previously described (Follett et al., 2000; Rosenberg et al., 2003). GalC polyclonal antiserum stained immature OL cell bodies and processes (Keirstead et al., 1998) and colocalized with O1 in double-staining experiments (data not shown). NeuN antibody labeled the majority of cortical and subcortical neurons, predominantly in the nucleus, and immunolabeling of cortical tissue with NSE antibody intensely stained neuronal cell bodies and processes (Mullen et al., 1992; Gao et al., 1999). Both GAD-65 and GABA antibodies demonstrated a similar expression pattern, staining most interneuron cell bodies and processes (Liu et al., 2003; Kultas-Ilinsky et al., 2004).

RESULTS

AMPAR subunit protein expression in the developing white matter from Long Evans rats

Western blot analysis of white matter homogenates demonstrated that in LE rats GluR1–GluR4 AMPAR subunits were expressed at all ages examined, although each subunit showed a distinct temporal expression pattern (Fig. 1). In the immature white matter, GluR1 and GluR2 subunit expression (Fig. 1A, B) was lower than in adulthood, whereas GluR3 and GluR4 subunits (Fig. 1C,D) largely superceded adult levels. GluR1 (Fig. 1A) was significantly lower than in the adult at P3 (approximately 18% of adult, $P < 0.02$), then increased gradually with maturation (45% at P7 and 49% at P11) and reached adult-like expression levels by P21 (109%). Similarly, GluR2 (Fig. 1B) was significantly lower than in the adult at P3 (approximately 20% of the adult level, $P < 0.001$) and remained low during

development (35% at P7, $P < 0.001$; 49% at P11, $P < 0.006$; 83% of adult at P21). In contrast, levels of GluR3 (Fig. 1C) were approximately 281% of adult at P3, became significantly higher than adult at P7 (424%, $P < 0.004$) and at P11 (358%, $P < 0.02$), and then declined to 179% by P21. GluR4 levels (Fig. 1D) were significantly higher than in the adult at P3 (749%, $P < 0.03$) and at P7 (1,289%, $P < 0.001$) and then dropped to 394% at P11 and 342% at P21. Maximal GluR4 levels at P7 were also significantly higher compared with P3 ($P < 0.04$) and P11 ($P < 0.002$).

Because higher non-GluR2/GluR2 ratios are associated with functionally increased Ca^{2+} permeability of the AMPAR (Pellegrini-Giampietro et al., 1992; Sanchez et al., 2001; Kumar et al., 2002), non-GluR2/GluR2 subunit ratios were calculated (see Materials and Methods) and compared among ages (Fig. 2). In white matter, GluR1/GluR2 ratios (Fig. 2A) demonstrated little variation at all ages examined (approximately 1:1–1.5:1) and were not significantly different from adult ratios (1:1). In contrast, GluR3/GluR2 and GluR4/GluR2 ratios were much higher at younger ages (P3 and P7) compared with adult ratios, and there was a progressive decrease with maturation (Fig. 2B,C). GluR3/GluR2 ratios (Fig. 2B) were significantly higher than in the adult at P3 (approximately 15:1, $P < 0.004$) and P7 (13:1, $P < 0.007$) and then dropped to 7:1 at P11 and 2:1 at P21. GluR4/GluR2 ratios (Fig. 2C) were also significantly higher than in the adult at P3 (41:1, $P < 0.02$) and P7 (38:1, $P < 0.02$), then decreased to 8:1 at P11 and to 4:1 at P21. Correspondingly, relative to the adult (3:1), total non-GluR2/GluR2 ratios (Fig. 2D) were significantly higher at P3 (56:1, $P < 0.008$) and P7 (52:1, $P < 0.009$) and then decreased to 16:1 at P11 and 8:1 at P21.

Cell-specific AMPAR subunit expression in the developing white matter from Long Evans rats

White matter Western blots indicated significantly higher AMPAR expression levels during the first and second postnatal weeks compared with adult levels. Because early increases in GluR3 and GluR4 expression at P3 and P7 were associated with a relative lack in GluR2 expression (Figs. 1, 2), we sought to determine which white matter components reflected this pattern. Therefore, we performed immunocytochemical double-labeling experiments for AMPAR subunits and glial-cell-specific markers in tissue sections from LE rat pups, during the same developmental window as analyzed by Western blot (P1– P21). Radial glia were identified by vimentin and GFAP staining, and astrocytes were visualized by GFAP labeling (Stichel et al., 1991). Oligodendrocytes were identified based on their immunoreactivity for stage-specific markers: O4 for OL precursors, GalC/O1 for immature OLs, and myelin basic protein (MBP) for mature OLs (Follett et al., 2000; Rosenberg et al., 2003; Craig et al., 2003).

Preliminary to determining the cell-specific AMPAR expression profile, we characterized white matter cellular development, using astroglial and OL stage-specific markers (Fig. 3). These revealed dramatic changes in the cellular population over the window of analysis. Between P1 and P5, the astrocytic lineage was represented mainly by radial glia. $GFAP^+$/$vimentin^+$ radial glia displayed distinct cell bodies located within the periventricular zone (PVZ) and extended long processes toward the pial surface (Fig. 3A1–C1). Only a few ramified $GFAP^+$/$vimentin^-$ astrocytes were present at this age and were located exclusively

near the ventricle wall. Between P7 and P9, radial glia fibers gradually disappeared, coincident with an increase in the population of GFAP$^+$/vimentin$^-$ astrocytes (Fig. 3D1–F1). The density of mature astrocytes within the white matter peaked at about P10–P12, before decreasing again at P14–P21 (data not shown). OL immu-nostaining showed that, at P1–P5, OL precursors (04$^+$/GalC$^-$), representing the major OL population at this age, were abundant and uniformly distributed throughout the white matter (Fig. 3A2–C2). At P7–P9, immature OLs (04$^+$/GalC$^+$) were the predominant OL stage (Fig. 3D2– F2), although MBP staining first became visible in the pericallosal white matter at this age (Fig. 3A3). Between P10 and P21, the MBP staining progressed in a medial-lateral/inside-outside gradient in the white matter fiber tracts and radiating cellular processes into the cortex (Fig. 3B3,C3).

We next evaluated the differential expression of AMPAR subunits on specific glial subtypes. The most dramatic changes in AMPAR expression level and subunit composition were observed during the first 2 postnatal weeks, consistently with the Western blot results. There were marked differences between developing astroglia and oligodendroglia, regarding both timing of presentation and receptor subunit composition. Radial glia were the earliest cell type in white matter to express AMPARs, with robust expression visible at P1–P5 (Fig. 4A1–L1). GluR1 was minimally expressed in astroglial lineage cells at all ages (Fig. 4A1–C1 and A2–C2) relative to neuronal cell types (see below). However, comparison across ages showed that GluR2 was minimal in radial glia at P1–5 (Fig. 4D1–F1) but highly expressed in mature astrocytes between P7 and P12 (Fig. 4D2–F2). In contrast, GluR3 and GluR4 were abundantly expressed on both radial glia at P1–P5 (Fig. 4G1–I1, J1–L1) as well as on astrocytes at P7–P12 (Fig. 4G2–I2, J2–L2) but started to decrease by P14 (data not shown).

Double labeling with AMPAR subunits and OL markers revealed little expression at P1–P5 on pre-OLs in LE rat brain (data not shown). However, AMPARs were highly expressed on pre-OLs between P7 and P9, and this was related primarily to expression of GluR4 (Fig. 5J1–L1). After P10, maturing OLs showed minimal to no GluR4 expression (Fig. 5J2–L2). Staining for GluR1, GluR2, and GluR3 was relative low or absent on pre-OLs at P1–P9 compared with surrounding cell types (Fig. 5A1–I1), and this relative lack of expression persisted from P10 (Fig. 5A2–I2) through P21 (data not shown). These findings are consistent with our previous observation that pre-OLs possess functional Ca^{2+}-permeable AMPARs at P7–P9 (Follett et al., 2000, 2004).

AMPAR subunit protein expression in the developing cortical gray matter from Long Evans rats

Western blot analysis of cortical samples demonstrated that, similar to the white matter, AMPAR subunits GluR1–GluR4 were expressed during the entire time window analyzed, but showed differential developmental trends (Fig. 6). GluR1 subunit expression exceeded adult levels from P3 through P21 (Fig. 6A), whereas GluR2, GluR3, and GluR4 were expressed at lower-than-adult levels (Fig. 6B – D). GluR1 expression (Fig. 6A) represented approximately 144% of adult expression at P3–P5 and was significantly higher than in the adult at P7–P9 (642%, $P < 0.001$), P11 (825%, $P < 0.001$), and P14–P21 (414%, $P < 0.004$). Unlike GluR1 levels, GluR2 levels (Fig. 6B) were significantly lower than in the adult at

P3–P5 (10%, $P < 0.001$), P7–P9 (27%, $P < 0.001$), and P11 (44%, $P < 0.004$) and then rose to approximately 72% of adult levels at P14–P21. GluR3 subunit expression (Fig. 6C) paralleled that of GluR2, being significantly lower than adult expression at P3–P5 (16%, $P < 0.001$), P7–P9 (25%, $P < 0.001$), and P11 (29%, $P < 0.001$) and then increasing to approximately 72% of adult expression at P14–P21. GluR4 levels (Fig. 6D) were significantly lower than in the adult at all ages examined: P3–P5 (14% of adult, $P < 0.001$), P7–P9 (26%, $P < 0.001$), P11 (33%, $P < 0.001$), and P14–P21 (70%, $P < 0.009$).

As in the white matter, non-GluR2/GluR2 ratios were calculated and compared among age groups (Fig. 7). GluR1/GluR2 ratios (Fig. 7A) were much higher at younger ages, compared with adult, showing an increase at P7–P9, followed by a progressive decrease with maturation. The GluR1/GluR2 ratio was about 14:1 at P3–P5, became significantly higher than in the adult at P7–P9 (28:1, $P < 0.03$), and then decreased gradually to 19:1 at P11 and 6:1 at P14–P21. In contrast, GluR3/GluR2 (Fig. 7B) and GluR4/GluR2 ratios (Fig. 7C) varied little with age (approximately 1:1–1.7:1) and therefore were not significantly different from adult ratios. Whereas total non-GluR2/GluR2 ratio (Fig. 7D) was approximately 3:1 in the adult, this ratio was higher at P3–P5 (approximately 17:1) and rose to significantly higher levels at P7–P9 (30:1, $P < 0.04$), before decreasing again to 20:1 at P11 and 8:1 at P21.

Cell-specific AMPAR subunit expression in the developing neocortex from Long Evans rats

In contrast to the white matter, where AMPAR expression peaked by the end of the first postnatal week (Fig. 1), Western blots of cortex showed maximal AMPAR expression later, during the second week of life (Fig. 6). Notably, high levels of GluR1 at P7–P14 in the developing cortex were associated with a significant relative deficiency in GluR2 expression compared with younger and older ages (Figs. 6, 7). To characterize the cellular distribution of this differential expression pattern, we performed immunocytochemical double labeling with GluR1–GluR4 subunit antibodies and neuronal markers NeuN, NSE, GAD-65, and γ-aminobutyric acid (GABA) in LE rats from P1 to P21. Subplate neurons and cortical plate neurons, stained with NeuN and NSE, were distinguished from one another based on the distribution pattern and cellular morphology, consistently with previous reports (Hanganu et al., 2002; Luhmann et al., 2003). Cortical pyramidal and nonpyramidal neurons were further distinguished by their GAD-65 and GABA immunoreactivity.

As in the white matter, first we characterized the developmental patterns of specific neuronal subpopulations in the cortex. In the first 2 postnatal weeks, the subcortical plate was located directly below the developing cortex and was populated by mostly horizontally oriented neurons at a low cellular density (Figs. 8, 9). In early postnatal development (P1–P5), the subplate region was only a thin layer of neurons (data not shown). By P7–P9, the subcortical plate was well formed and of full thickness (Fig. 8A), appeared to be slightly decreased at P10–P12 (Fig. 8B), and then gradually disappeared by P14–P21 (Fig. 8C). In contrast, the cortical plate thickness increased steadily from P1 through P21 (Fig. 8A – C), and starting by P10–P12 all cortical layers were distinguishable (Fig. 8B,C).

Cell-specific AMPAR subunit expression was examined in subplate and cortex. Subplate neurons were the first cell type to express AMPARs. Between P1 and P9, subplate neurons showed expression of GluR1 and GluR4 (Fig. 9A1–C1, J1–L1), whereas little to no GluR2 or GluR3 was present (Fig. 9D1–F1, G1–I1). At P10–P12, subplate neurons acquired GluR2 and GluR3 expression (Fig. 9D2–F2, G2–I2), although the expression of GluR1 and GluR4 did not appreciably change during the first 2 postnatal weeks (Fig. 9A2– C2, J2–L2). Between P14 and P21, GluR1 and GluR4 expression decreased on the remaining subplate neurons, as the population diminished, while GluR2 and GluR3 levels remained elevated (data not shown).

Prior to the second postnatal week, pyramidal and nonpyramidal cortical neurons expressed little to no AMPARs. GluR1 was the first subunit to appear in this population and was weakly positive by P7 on layer V pyramidal neurons (data not shown). Pyramidal neuron GluR1 expression increased during the second postnatal week, peaking at P10–P12 (Fig. 10A1–C1), compared with younger and older ages (Fig. 10A2–C2). In contrast, GluR2 and GluR3 were minimally expressed on pyramidal neurons from P1 through P12 (Fig. 10D1–F1, G1–I1) but became evident at P14–P21 (Fig. 10D2–F2, G2–I2). Pyramidal neuron GluR4 expression was low at all ages compared with glial cells or other neuronal subtypes (Fig. 10J1–L1, J2–L2).

Double labeling with GAD-65 or GABA and AMPAR subunits revealed minimal expression of AMPARs on nonpyramidal neurons prior to P10–P12 (data not shown). At P10, nonpyramidal neurons labeled for GluR1, GluR3, and GluR4 subunits (Fig. 11A1–C1, G1–I1, J1–L1), and staining for all three subunits appeared to increase by P21 (Fig. 11A2–C2, G2–I2, J2–L2). Strikingly, GluR2 expression on nonpyramidal neurons was low at all ages relative to other cell types and did not increase with age (Fig. 11D1–F1, D2–F2).

Strain-specific differences in temporal onset of AMPAR subunit expression: a comparison study between Sprague Dawley and Long Evans rats

The developmental profile of regional susceptibility to H/I varies in models using different rat strains (Jensen et al., 1991; Sheldon et al., 1996; Owens et al., 1997; Follett et al., 2000; Cai et al., 2001; Back et al., 2002). We therefore compared the temporal and regional developmental expression of AMPARs between LE and SD rats, two widely used strains for animal model studies. We examined the developmental patterns of specific AMPAR white matter subunits on all cell types, with a particular interest on OLs and cortical neurons, because AMPARs on these cell types have been postulated as critical for H/I pathophysiology in white matter and gray matter. We first analyzed the differences in white matter and cortical cellular maturation and then examined strain-specific differences in AMPAR subunit expression.

As described earlier, white matter maturation was assessed by differential expression of astroglial-stage-specific (vimentin, GFAP) and OL-stage-specific (O4, O1, GalC, and MBP) markers. In contrast to LE rats, in which vimentin^{+}/GFAP^{+} radial glia represented the major astroglial population in the white matter prior to P7–P9 (Fig. 3A1–C1), there was a significant increase in vimentin^{-}/GFAP^{+} mature astrocytes already at P3 in SD rats (Fig. 12A1–C1). However, by P7 there was no significant difference between both strains (Figs.

3D1–F1, 12D1–F1). OL-lineage marker antibodies demonstrated the same earlier progression in SD compared with LE rats. In LE rats, only scattered $O4^+/GalC^+$ immature OL were observed in the pericallosal white matter between P1 and P5 (Fig. 3A2–C2), whereas $O4^+/GalC^+$ OLs were substantially more abundant in SD rats of the same age (Fig. 12A2–C2). At P7, immature ($O4^+/GalC^+$) OLs predominated in both LE (Fig. 3D2–F2) and SD (Fig. 12D2–F2) rats. Interestingly, the earliest onset of MBP expression was first observed in OL cell bodies in the pericallosal white matter at P7 in both strains (data not shown).

With respect to AMPAR subunit expression, in both LE and SD rats, GluR4 and GluR2 subunits on developing astroglia followed a similar expression pattern. GluR4 was expressed on both $vimentin^+/GFAP^+$ radial glia and $vimentin^-/GFAP^+$ differentiated astrocytes. However, GluR2 was not expressed in radial glia and increased with maturation on differentiated astrocytes. Relative to LE rats, $GluR2^+$ astrocytes were already seen in SD rats at P5 (data not shown). OLs in SD rats showed robust GluR4 staining at P3 and P7 (Fig. 13D – I), in contrast to LE rats, in which high GluR4 expression was first observed at P6–P7 (Fig. 5J1–L1). In both strains, GluR4 levels were decreased by P10 and P14. Similar to LE rats, GluR2 expression on $O4^+$ OLs in the SD rat was low at all ages analyzed (data not shown).

Differences in cortical development between strains were assessed by comparing age-dependent neuronal laminar patterns, visualized via NeuN immunostaining (data not shown). Consistent with differences in white matter maturation, SD rats revealed an earlier appearance and expansion of all six cortical layers coincident with a marked decrease of the subplate by P7, although these changes were not seen until P10 in the LE rat.

Differences in AMPAR expression between the two strains were also apparent in subplate and cortical neurons. In contrast to LE rats, in which subplate neurons at P7 showed robust expression of GluR2-lacking AMPARs (see Fig. 9), the peak expression of GluR2-lacking AMPARs occurred earlier, at P3–P5, in SD rats (data not shown). In SD rats, GluR1 subunit was highly expressed on pyramidal and nonpyramidal neurons at P7 (Fig. 14D1–F1), whereas in LE rats high GluR1 expression was not observed until P10–P12 (Fig. 10A1–C1). Likewise, in SD rats, GluR2 subunit was apparent on pyramidal neurons at P10 (Fig. 14G2–I2), in contrast to the case in LE rats, in which GluR2 was low at P11 (Fig. 8D1–F1) and first became visible between P14 and P21 (Fig. 8D2–F2).

DISCUSSION

The present study details the developmental regulation of regional and cellular AMPAR subunit expression in rodent cerebrum. In both white and gray matter, there are transient periods of development in which AMPARs 1) supercede adult levels and 2) exhibit a relative GluR2 deficiency, consistent with a Ca^{2+}-permeable state. The present study is the first to investigate the cellular distribution and temporal regulation of all AMPAR subunits in the developing white matter and cortex and to evaluate specifically the differential expression of GluR2-lacking AMPARs on all glial and neuronal subtypes during the first 3 postnatal weeks in rat. During the first postnatal week, GluR2-lacking AMPARs were

expressed predominantly on white matter cellular elements, including radial glia, pre-OLs, and subplate neurons, whereas, during subsequent development, these AMPARs were highly expressed on cortical neurons, coincident with decreased expression on white matter cells. In both white and gray matter, the periods of high GluR2 deficiency correspond to those of regional susceptibility to H/I injury, supporting prior studies suggesting a critical role for Ca^{2+}-permeable AMPARs in excitotoxic cellular injury and epileptogenesis. Furthermore, the developmental regulation of these receptor subunits strongly suggests that Ca^{2+} influx through GluR2-lacking AMPARs may play an important role in neuronal and glial differentiation as well as myelination of the immature brain.

Potential role of Ca^{2+}-permeable AMPARs in regional selectivity of H/I injury during development

The AMPA subtype of glutamate receptors are widely expressed on developing neurons and glia and have been postulated as critical for certain forms of perinatal H/I brain injury and seizures (Pellegrini-Giampietro et al., 1992). In P7 rats, systemic administration of AMPAR antagonists are highly protective against H/I injury to developing OLs (Follett et al., 2000, 2004) and can significantly reduce H/I cortical neuronal injury (Hagberg et al., 1994). Similarly, treatment with specific AMPAR antagonists, rather than NMDAR antagonists or GABAR agonists, is highly effective in suppressing hypoxia-induced seizures in P10–P12 rats and prevents later increases in seizure-induced neuronal injury (Jensen et al., 1995; Koh and Jensen, 2001; Koh et al., 2004).

Further support for an excitotoxic role for Ca^{2+}-permeable AMPARs is derived from in vitro data. In OL cultures, susceptibility to AMPAR-mediated cell death is developmentally regulated. Immature OLs in culture express Ca^{2+}-permeable AMPARs (Itoh et al., 2002; Deng et al., 2003; Rosenberg et al., 2003). Immature OLs, but not mature OLs, are highly susceptible to both oxygen glucose deprivation (OGD) and direct AMPA/KA receptor-mediated toxicity (Fern and Moller, 2000; Deng et al., 2003; Rosenberg et al., 2003) The same age dependence in vulnerability to AMPA toxicity was observed in neuronal cultures, which correlates with the expression of Ca^{2+}-permeable AMPARs (Jensen et al., 1998b, 2001). In neurons, in addition to mediating excitotoxicity, Ca^{2+} influx through GluR2-lacking AMPAR has been implicated in developmental synaptic plasticity and epileptogenesis (Gu et al., 1996; Sanchez et al., 2001, 2005). In contrast to immature OLs and neurons, cultured astrocytes are more resistant to H/I or AMPA/KA receptor-mediated excitotoxicity (Lyons and Kettenmann, 1998; Yamaya et al., 2002), and this may be due to expression of AMPARs with lower Ca^{2+} permeability (Yamaya et al., 2002).

Developmental regulation of AMPAR subunit expression in the rodent white matter

Our data demonstrate that, in the white matter, all four AMPAR subunits were expressed as early as P3, but each subunit showed different postnatal changes. During the first 2 postnatal weeks, GluR4 and GluR3 expression transiently exceeded the adult levels, peaking at about P7, in contrast to GluR1 and GluR2 subunits expressed below the adult levels. Moreover, total non-GluR2/GluR2 ratios peaked between P3 and P7, suggesting that the highest levels of GluR2-lacking AMPARs are transiently expressed in the developing white matter during the first postnatal week, the time of greatest susceptibility to H/I white matter injury.

Consistent with an "inside-out" gradient, the first cells to express AMPARs in white matter were the radial glia. Between P1 and P5, radial glia possesses AMPARs composed of GluR3 and GluR4 subunits, with minimal GluR1 or GluR2. This novel finding suggests that Ca^{2+}-permeable (GluR2-lacking) AMPARs might be transiently expressed on cerebral radial glia in situ and is consistent with previous in vitro observations (Lopez et al., 1994). Recent studies have demonstrated that at the time of neurogenesis these cells can themselves generate neurons, in addition to providing guidance for neuronal migration toward the developing cortical plate (Noctor et al., 2001, 2002; Tamamaki et al., 2001). After birth, when neuronal migration is complete, radial glia transform into astrocytes and also migrate to the overlying structures (Takahashi et al., 1990; Gressens et al., 1992). Ca^{2+} influx into radial glia via AMPARs may influence these complex maturational events. On the other hand, the presence of Ca^{2+}-permeable AMPARs may render radial glia more susceptible to excitotoxic or traumatic injury and may play a role in the formation of laminar or focal cortical dysgenesis (Gressens et al., 1992; Super et al., 2000; Levison et al., 2001).

Mature astrocytes demonstrated robust GluR2 subunit expression starting around P7, coincident with their morphological transformation from immature cells (i.e., radial glia). These results indicate that, similar to hippocampal astrocytes (Seifert and Steinhauser, 1995; Seifert et al., 1997), white matter astrocytes may possess AMPARs with low Ca^{2+} permeability, which may explain the relative resistance of this cell type to H/I injury.

A different expression pattern was observed in pre-OLs. At about P7, GluR4 containing AMPARs were transiently expressed on pre-OLs, as previously reported by us and others (Ong et al., 1996; Follett et al., 2000). Similar to radial glia, but in contrast to astrocytes, GluR2 expression in pre-OLs was relatively low, which correlates with functional studies demonstrating that AMPARs expressed on developing OLs display increased Ca^{2+} permeability (Fulton et al., 1992; Bergles et al., 2000; Itoh et al., 2002; Deng et al., 2003; Follett et al., 2004). In contrast, mature MBP^{+} OLs express low levels of AMPARs, including GluR2, and are relatively resistant to AMPAR-mediated and H/I injury in vitro and in vivo (Follett et al., 2000; Deng et al., 2003; Rosenberg et al., 2003). The presence of GluR2-lacking AMPARs in pre-OLs in situ correlates closely with observations of protective efficacy of AMPAR antagonists in selective H/I white matter injury in the first postnatal week (Follett et al., 2000, 2004). Furthermore, their presence on migrating pre-OLs raises the intriguing possibility that glutamate may be playing a trophic or chemotactant role in OL process guidance. Indeed, glutamate and glutamate receptor antagonists have been shown to have potent effects on differentiation and migration of pre-OLs in vitro (Gallo et al., 1996; Yuan et al., 1998).

Developmental regulation of AMPAR subunit expression in the rodent cortical gray matter

In the cortex, GluR1–GluR4 subunits were also expressed as early as P3. GluR1 expression was significantly higher than in adult during the entire developmental window analyzed (P3–P21), peaking at P10–P12. In contrast, GluR2, GluR3, and GluR4 subunits increased progressively with age but were still expressed at lower-than-adult levels by P21. Consequently, GluR1/GluR2 and total non-GluR2/GluR2 ratios were significantly higher between P7 and P9, compared with adult ratios, consistent with increased expression of

GluR2-lacking AMPARs in the developing cortex during the second postnatal week, the interval of greatest neuronal susceptibility to H/I.

As in white matter, expression of AMPARs during cortical development followed an "inside-out" gradient. Cortical AMPAR expression began later than that in white matter, and the subplate neurons were the first cells to express AMPARs within cortex. These findings are consistent with the observation that electrophysiological AMPAR responses are observed earlier on subplate neurons compared with cortical neurons in situ in perinatal rats (Hanganu et al., 2002; Luhmann et al., 2003). By the end of the first postnatal week (P7), GluR1- and GluR4-containing AMPARs were highly expressed on subplate neurons, whereas GluR2 and GluR3 levels were low, suggesting that these receptors might be Ca^{2+} permeable during early postnatal life. The subcortical plate represents a transient structure, with subplate neurons and newly migrated cortical plate neurons forming a complex network (Friauf et al., 1990; Friauf and Shatz, 1991). This early transitional cortical network may play an important role in the development of cortical excitatory and inhibitory connections (Ghosh and Shatz, 1993; Kanold et al., 2003). The transient expression of Ca^{2+}-permeable AMPARs on subplate neurons may contribute to heightened synaptogenesis and synaptic plasticity during this critical period of development. At the same time, these receptors may contribute to selective vulnerability of sub-plate neurons to H/I or excitotoxic injury (Lein et al., 1999; Super et al., 2000; McQuillen et al., 2003) and might underlie the disruptive effects of deep cortical injury during the first postnatal week on subsequent cortical organization and excitability (Ghosh and Shatz, 1993; Lein et al., 1999; Super et al., 2000).

Cortical pyramidal neurons exhibited a similar developmental lag in GluR2 and GluR3 expression relative to GluR1. GluR1 expression was most prominent around P10, whereas GluR2 and GluR3 subunit expression became apparent later, between P14 and P21. Our finding that GluR2-lacking (Ca^{2+}-permeable) AMPARs are transiently expressed on cortical pyramidal neurons during the second postnatal week is in agreement with previous reports showing the functional presence of these receptors on pyramidal neurons in brain slices removed from P10–P14 rats (Sanchez et al., 2001; Kumar et al., 2002). The role of these receptors in excitotoxicity, synaptogenesis, and plasticity in the immature brain is unknown. However, AMPARs have been shown to be critical for the epileptogenic effects of hypoxia in the P10–P12 rat pup (Jensen et al., 1995, 1998a; Koh and Jensen, 2001; Sanchez et al., 2001, 2005; Koh et al., 2004). It appears that specific signaling pathways downstream from these Ca^{2+}-permeable receptors on pyramidal neurons in the developing rodent brain induce functional changes in neuronal excitability and synaptic plasticity (Sanchez et al., 2001, 2005). Furthermore, AMPAR antagonists selectively block the epileptogenic effects of hypoxia and attenuate cortical injury in developing brain (Hagberg et al., 1994; Koh and Jensen, 2001; Koh et al., 2004).

A different expression pattern was observed in inter-neurons. Despite significant increases in GluR2 expression on pyramidal neurons between P14 and P21, the majority of interneurons continued to show a relative lack of GluR2, suggesting the persistence of Ca^{2+}-permeable AMPARs. These findings support a large number of studies showing that, in the adult brain, mature interneurons possess functional Ca^{2+}-permeable AMPARs with inwardly

rectifying current-voltage (I-V) relationships and glutamate-agonist-induced Ca^{2+} entry (Hestrin, 1993; Jonas et al., 1994). It has been postulated that the interneurons are protected from excitotoxicity, in part because of high intracellular levels of Ca^{2+}-binding proteins, such as calbindin (Goodman et al., 1993). Notably, in the first 2 postnatal weeks, interneurons possess significantly lower levels of Ca^{2+}-binding proteins compared with adult levels (Alcantara et al., 1993) and therefore may be selectively vulnerable to H/I injury. Indeed, induced status epilepticus in the immature brain results in prominent interneuronal injury (da Silva et al., 2005), and H/I in the first postnatal weeks decreases interneuron density later in life (Goodman et al., 1993).

Strain-dependent differences in temporal profile of AMPAR subunit development

This is the first study to perform a detailed analysis of AMPAR subunit expression differences between two widely used rat strains. These data show that, in SD rats, GluR2-lacking AMPARs were maximally expressed on white matter OLs at P3–P5, whereas LE rats showed high levels of GluR2-lacking AMPARs on OLs at P6–P7. Likewise, the loss of GluR2-lacking radial glia occurred after P3 in SD rats but not until after P5 in LE rats. A similar maturational leftward shift for AMPARs in SD compared with LE rats was observed for subplate and cortical neurons. In SD rats, there was a peak of GluR1 expression in association with a relative GluR2 deficiency on subplate neurons at P3–P5 and on cortical neurons between P7 and P9 compared with later ages. By contrast, in LE rats, this pattern occurred around P7 on subplate neurons and between P10 and P12 on cortical neurons. Overall, the SD rats appeared for a given chronological age to be approximately 2–3 days more mature with respect to cell lineage changes and AMPAR expression than the LE rats. This discrepancy helps to explain modest differences in stated susceptibility windows in rodent H/I and epilepsy model literature. For example, the selectivity of H/I injury for white matter between P1 and P3 has been reported for SD rats (Back et al., 2002; McQuillen et al., 2003), whereas, in LE rats, the window of greatest vulnerability of white matter to H/I and glutamate agonist injection is P6–P7 (Follett et al., 2000). Similarly, several studies report that the P7 SD rat shows severe cortical injury when exposed to H/I (Andine et al., 1990; Grafe, 1994), whereas, in the LE rat, there is maximal injury at P10–P12 (Jensen et al., 1994; Chen et al., 1998). Likewise, hypoxia causes seizures in LE rats at P10 (Jensen et al., 1991) but not at earlier ages, and seizures are best elicited by hypoxia at P8 in SD rats (Owens et al., 1997). In understanding these strain differences, it is important to consider the effect of gestational age. The average gestation for LE rats is 21 days, whereas gestation in the SD rat is 23 days. Hence the reported 2–3-day lag between the two strains may well be simply due to differences in the duration of gestation, such that, for example, a P6–P7 LE rat has a postconceptional age equivalent to that of a P3–P5 SD rat. The differences in AMPAR expression between the two strains thus vanish if postconceptional age is the critical variable. Nevertheless, differences in AMPAR subunit progression between the strains have important implications when evaluating specific ages with respect to their suitability for modeling human disease and development. Moreover, it is likely that other rat strains will show different patterns of variation, and this study suggests that such comparisons might have to be made on a case-by-case basis.

Acknowledgments

Grant sponsor: William Randolph Hearst Foundation (to D.M.T.); Grant sponsor: Epilepsy Foundation (to D.M.T.); Grant sponsor: National Institute of Neurological Disorders and Stroke; Grant number: NS31718 (to F.E.J., R.E.F.); Grant sponsor: The Korean Science Foundation (to H.P.); Grant sponsor: National Institutes of Health; Grant number: NS38475 (to J.J.V., F.E.J.); Grant number: HD01359 (to P.L.F.); Grant sponsor: United Cerebral Palsy Foundation (to F.E.J.); Grant sponsor: Charles H. Hood Foundation (to P.L.F.); Grant sponsor: Mental Retardation Research Center Grant (National Institute of Child Health and Human Development): Grant number: P30 HD18655.

LITERATURE CITED

Alcantara S, Ferrer I, Soriano E. Postnatal development of parvalbumin and calbindin D28K immunoreactivities in the cerebral cortex of the rat. Anat Embryol. 1993; 188:63–73. [PubMed: 8214625]

Andine P, Thordstein M, Kjellmer I, Nordborg C, Thiringer K, Wennberg E, Hagberg H. Evaluation of brain damage in a rat model of neonatal hypoxic-ischemia. J Neurosci Methods. 1990; 35:253–260. [PubMed: 2084395]

Andine P, Sandberg M, Bagenholm R, Lehmann A, Hagberg H. Intra- and extracellular changes of amino acids in the cerebral cortex of the neonatal rat during hypoxic-ischemia. Brain Res Dev Brain Res. 1991; 64:115–120.

Back SA, Han BH, Luo NL, Chricton CA, Xanthoudakis S, Tarn J, Arvin KL, Holtzman DM. Selective vulnerability of late oligodendrocyte progenitors to hypoxia-ischemia. J Neurosci. 2002; 22:455–463. [PubMed: 11784790]

Banker BQ, Larroche JC. Periventricular leukomalacia of infancy. A form of neonatal anoxic encephalopathy. Arch Neurol. 1962; 7:386–410. [PubMed: 13966380]

Benveniste H, Drejer J, Schousboe A, Diemer NH. Elevation of the extracellular concentrations of glutamate and aspartate in rat hippocampus during transient cerebral ischemia monitored by intracerebral microdialysis. J Neurochem. 1984; 4:1369–1374. [PubMed: 6149259]

Bergles DE, Roberts JD, Somogyi P, Jahr CE. Glutamatergic synapses on oligodendrocyte precursor cells in the hippocampus. Nature. 2000; 405:187–191. [PubMed: 10821275]

Burnashev N, Monyer H, Seeburg PH, Sakmann B. Divalent ion permeability of AMPA receptor channels is dominated by the edited form of a single subunit. Neuron. 1992; 8:189–198. [PubMed: 1370372]

Cai Z, Pang Y, Xiao F, Rhodes PG. Chronic ischemia preferentially causes white matter injury in the neonatal rat brain. Brain Res. 2001; 898:126–135. [PubMed: 11292456]

Chen HS, Wang YF, Rayudu PV, Edgecomb P, Neill JC, Segal MM, Lipton SA, Jensen FE. Neuroprotective concentrations of the N-methyl-D-aspartate open-channel blocker memantine are effective without cytoplasmic vacuolation following post-ischemic administration and do not block maze learning or long-term potentiation. Neuroscience. 1998; 86:1121–1132. [PubMed: 9697119]

Conti F, Minelli A, Molnar M, Brecha NC. Cellular localization and laminar distribution of NMDAR1 mRNA in the rat cerebral cortex. J Comp Neurol. 1994; 343:554–565. [PubMed: 8034787]

Craig A, Ling LN, Beardsley DJ, Wingate-Pearse N, Walker DW, Hohimer AR, Back SA. Quantitative analysis of perinatal rodent oligodendrocyte lineage progression and its correlation with human. Exp Neurol. 2003; 181:231–240. [PubMed: 12781996]

da Silva AV, Regondi MC, Cavalheiro EA, Spreafico R. Disruption of cortical development as a consequence of repetitive pilocarpine-induced status epilepticus in rats. Epilepsia. 2005; 46(Suppl 5):22–30. [PubMed: 15987249]

Deng W, Rosenberg PA, Volpe JJ, Jensen FE. Calcium-permeable AMPA/kainate receptors mediate toxicity and preconditioning by oxygen-glucose deprivation in oligodendrocyte precursors. Proc Natl Acad Sci U S A. 2003; 100:6801–6806. [PubMed: 12743362]

Fern R, Moller T. Rapid ischemic cell death in immature oligodendrocytes: a fatal glutamate release feedback loop. J Neurosci. 2000; 20:34–42. [PubMed: 10627578]

Ferriero DM. Neonatal brain injury. N Engl J Med. 2004; 351:1985–1995. [PubMed: 15525724]

Follett PL, Rosenberg PA, Volpe JJ, Jensen FE. NBQX attenuates excitotoxic injury in developing white matter. J Neurosci. 2000; 20:9235–9241. [PubMed: 11125001]

Follett PL, Deng W, Dai W, Talos DM, Massillon LJ, Rosenberg PA, Volpe JJ, Jensen FE. Glutamate receptor-mediated oligodendrocyte toxicity in periventricular leukomalacia: a protective role for topiramate. J Neurosci. 2004; 24:4412–4420. [PubMed: 15128855]

Friauf E, Shatz CJ. Changing patterns of synaptic input to subplate and cortical plate during development of visual cortex. J Neurophysiol. 1991; 66:2059–2071. [PubMed: 1812236]

Friauf E, McConnell SK, Shatz CJ. Functional synaptic circuits in the subplate during fetal and early postnatal development of cat visual cortex. J Neurosci. 1990; 10:2601–2613. [PubMed: 2388080]

Friedman LK, Koudinov AR. Unilateral GluR2(B) hippocampal knockdown: a novel partial seizure model in the developing rat. J Neurosci. 1999; 19:9412–9425. [PubMed: 10531445]

Fulton BP, Burne JF, Raff MC. Visualization of 0-2A progenitor cells in developing and adult rat optic nerve by quisqualate-stimulated cobalt uptake. J Neurosci. 1992; 12:4816–4833. [PubMed: 1281496]

Gallo V, Patneau DK, Mayer ML, Vaccarino FM. Excitatory amino acid receptors in glial progenitor cells: molecular and functional properties. Glia. 1994; 11:94–101. [PubMed: 7927651]

Gallo V, Zhou JM, McBain CJ, Wright P, Knutson PL, Armstrong RC. Oligodendrocyte progenitor cell proliferation and lineage progression are regulated by glutamate receptor-media ted K^+ channel block. J Neurosci. 1996; 16:2659–2670. [PubMed: 8786442]

Gao PP, Yue Y, Cerretti DP, Dreyfus C, Zhou R. Ephrin-dependent growth and pruning of hippocampal axons. Proc Natl Acad Sci U S A. 1999; 96:4073–4077. [PubMed: 10097165]

Gard AL, Pfeiffer SE. Oligodendrocyte progenitors isolated directly from developing telencephalon at a specific phenotypic stage:myelinogenic potential in a defined environment. Development. 1989; 106:119–132. [PubMed: 2697546]

Ghosh A, Shatz CJ. A role for subplate neurons in the patterning of connections from thalamus to neocortex. Development. 1993; 117:1031–1047. [PubMed: 8325233]

Goodman JH, Wasterlain CG, Massarweh WF, Dean E, Sollas AL, Sloviter RS. Calbindin-D28k immunoreactivity and selective vulnerability to ischemia in the dentate gyrus of the developing rat. Brain Res. 1993; 606:309–314. [PubMed: 8490723]

Grafe MR. Developmental changes in the sensitivity of the neonatal rat brain to hypoxic/ischemic injury. Brain Res. 1994; 653:161–166. [PubMed: 7982049]

Gressens P, Richelme C, Kadhim HJ, Gadisseux JF, Evrard P. The germinative zone produces the most cortical astrocytes after neuronal migration in the developing mammalian brain. Biol Neonate. 1992; 61:4–24. [PubMed: 1373658]

Grunert U, Lin B, Martin PR. Glutamate receptors at bipolar synapses in the inner plexiform layer of primate retina: light microscopic analysis. J Comp Neurol. 2003; 466:136–147. [PubMed: 14515245]

Gu JG, Albuquerque CJ, Lee CJ, MacDermott AB. Synaptic strengthening through activation of Ca^{2+}-permeable AMPA receptors. Nature. 1996; 381:793–796. [PubMed: 8657283]

Hagberg H. Hypoxic-ischemic damage in the neonatal rat brain: excitatory amino acids. Dev Pharmacol Ther. 1992; 18:139–144. [PubMed: 1306803]

Hagberg H, Gilland E, Deimer N, Andine P. Hypoxic-ischemic damage in the neonatal rat brain: histopathology after post-treament with NMDA and non-NMDA receptor antagonists. Biol Neonate. 1994; 66:213.

Hanganu IL, Kilb W, Luhmann HJ. Functional synaptic projections onto subplate neurons in neonatal rat somatosensory cortex. J Neurosci. 2002; 22:7165–7176. [PubMed: 12177212]

Hauser WA, Annegers JF, Kurland LT. Incidence of epilepsy and unprovoked seizures in Rochester, Minnesota: 1935–1984. Epilepsia. 1993; 34:453–468. [PubMed: 8504780]

Hestrin S. Different glutamate receptor channels mediate fast excitatory synaptic currents in inhibitory and excitatory cortical neurons. Neuron. 1993; 11:1083–1091. [PubMed: 7506044]

Hollmann M, Heinemann S. Cloned glutamate receptors. Annu Rev Neurosci. 1994; 17:31–108. [PubMed: 8210177]

Itoh T, Beesley J, Itoh A, Cohen AS, Kavanaugh B, Coulter DA, Grinspan JB, Pleasure D. AMPA glutamate receptor-media ted calcium signaling is transiently enhanced during development of oligodendrocytes. J Neurochem. 2002; 81:390–402. [PubMed: 12064486]

Jensen FE, Applegate CD, Holtzman D, Belin TR, Burchfiel JL. Epileptogenic effect of hypoxia in the immature rodent brain. Ann Neurol. 1991; 29:629–637. [PubMed: 1909851]

Jensen FE, Gardner G, Williams AP, Gallop P, Tang L, Aizenman E, Rosenberg P. In vivo neuroprotection of pyrroloquinoline quinone (PQQ) in a rodent stroke model. Neuroscience. 1994; 62:399–406. [PubMed: 7830887]

Jensen FE, Alvarado S, Firkusny IR, Geary C. NBQX blocks the acute and late epileptogenic effects of perinatal hypoxia. Epilepsia. 1995; 36:966–972. [PubMed: 7555960]

Jensen FE, Wang C, Stafstrom CE, Liu Z, Geary C, Stevens MC. Acute and chronic increases in excitability in rat hippocampal slices after perinatal hypoxia in vivo. J Neurophysiol. 1998a; 79:73–81. [PubMed: 9425178]

Jensen JB, Lund TM, Timmermann DB, Schousboe A, Pickering DS. Role of GluR2 expression in AMPA-induced toxicity in cultured murine cerebral cortical neurons. J Neurosci Res. 2001; 65:267–277. [PubMed: 11494361]

Jensen JB, Schousboe A, Pickering DS. Development of calcium-permeable alpha-amino-3-hydroxy-5-methyl-4-isoxazolepropionic acid receptors in cultured neocortical neurons visualized by cobalt staining. J Neurosci Res. 1998b; 54:273–281. [PubMed: 9788286]

Jonas P, Racca C, Sakmann B, Seeburg PH, Monyer H. Differences in Ca^{2+} permeability of AMPA-type glutamate receptor channels in neocortical neurons caused by differential expression of the GluR-B subunit. Neuron. 1994; 12:1281–1289. [PubMed: 8011338]

Kanold PO, Kara P, Reid RC, Shatz CJ. Role of subplate neurons in functional maturation of visual cortical columns. Science. 2003; 301:521–525. [PubMed: 12881571]

Keirstead HS, Levine JM, Blakemore WF. Response of the oligodendrocyte progenitor cell population (defined by NG2 labelling) to demy-elination of the adult spinal cord. Glia. 1998; 22:161–170. [PubMed: 9537836]

Koh S, Jensen FE. Topiramate blocks perinatal hypoxia-induced seizures in rat pups. Ann Neurol. 2001; 50:366–372. [PubMed: 11558793]

Koh S, Tibayan FD, Simpson J, Jensen FE. NBQX or topiramate treatment following perinatal hypoxia-induced seizures prevents later increases in seizure-induced neuronal injury. Epilepsia. 2004; 45:569–575. [PubMed: 15144420]

Kultas-Ilinsky K, Fallet C, Verney C. Development of the human motor-related thalamic nuclei during the first half of gestation, with special emphasis on GABAergic circuits. J Comp Neurol. 2004; 476:267–289. [PubMed: 15269970]

Kumar SS, Bacci A, Kharazia V, Huguenard JR. A developmental switch of AMPA receptor subunits in neocortical pyramidal neurons. J Neurosci. 2002; 22:3005–3015. [PubMed: 11943803]

Lein ES, Finney EM, McQuillen PS, Shatz CJ. Subplate neuron ablation alters neurotrophin expression and ocular dominance column formation. Proc Natl Acad Sci U S A. 1999; 96:13491–13495. [PubMed: 10557348]

Levison SW, Rothstein RP, Romanko MJ, Snyder MJ, Meyers RL, Van-nucci SJ. Hypoxia/ischemia depletes the rat perinatal subventricular zone of oligodendrocyte progenitors and neural stem cells. Dev Neurosci. 2001; 23:234–247. [PubMed: 11598326]

Lindahl JS, Keifer J. Glutamate receptor subunits are altered in forebrain and cerebellum in rats chronically exposed to the NMDA receptor antagonist phencyclidine. Neuropsychopharmacology. 2004; 29:2065–2073. [PubMed: 15138442]

Liu S, Wang J, Zhu D, Fu Y, Lukowiak K, Lu YM. Generation of functional inhibitory neurons in the adult rat hippocampus. J Neurosci. 2003; 23:732–736. [PubMed: 12574400]

Liu Y, Silverstein FS, Skoff R, Barks JD. Hypoxic-ischemic oligodendroglial injury in neonatal rat brain. Pediatr Res. 2002; 51:25–33. [PubMed: 11756636]

Loeliger M, Watson CS, Reynolds JD, Penning DH, Harding R, Bocking AD, Rees SM. Extracellular glutamate levels and neuropathology in cerebral white matter following repeated umbilical cord occlusion in the near term fetal sheep. Neuroscience. 2003; 116:705–714. [PubMed: 12573713]

Lopez T, Lopez-Colome AM, Ortega A. AMPA/KA receptor expression in radial glia. Neuroreport. 1994; 5:504–506. [PubMed: 8003684]

Luhmann HJ, Hanganu I, Kilb W. Cellular physiology of the neonatal rat cerebral cortex. Brain Res Bull. 2003; 60:345–353. [PubMed: 12781323]

Lyons SA, Kettenmann H. Oligodendrocytes and microglia are selectively vulnerable to combined hypoxia and hypoglycemia injury in vitro. J Cereb Blood Flow Metab. 1998; 18:521–530. [PubMed: 9591844]

Maller AI, Hankins LL, Yeakley JW, Butler IJ. Rolandic type cerebral palsy in children as a pattern of hypoxic-ischemic injury in the full-term neonate. J Child Neurol. 1998; 13:313–321. [PubMed: 9701479]

McQuillen PS, Sheldon RA, Shatz CJ, Ferriero DM. Selective vulnerability of subplate neurons after early neonatal hypoxia-ischemia. J Neurosci. 2003; 23:3308–3315. [PubMed: 12716938]

Michaelis EK. Molecular biology of glutamate receptors in the central nervous system and their role in excitotoxicity, oxidative stress, and aging. Prog Neurobiol. 1998; 54:369–415. [PubMed: 9522394]

Miyata T, Kawaguchi A, Okano H, Ogawa M. Asymmetric inheritance of radial glial fibers by cortical neurons. Neuron. 2001; 31:727–741. [PubMed: 11567613]

Moga DE, Janssen WG, Vissavajjhala P, Czelusniak SM, Moran TM, Hof PR, Morrison JH. Glutamate receptor subunit 3 (GluR3) immunoreactivity delineates a subpopulation of parvalbumin-containing in-terneurons in the rat hippocampus. J Comp Neurol. 2003; 462:15–28. [PubMed: 12761821]

Mullen RJ, Buck CR, Smith AM. NeuN, a neuronal specific nuclear protein in vertebrates. Development. 1992; 116:201–211. [PubMed: 1483388]

Noctor SC, Flint AC, Weissman TA, Dammerman RS, Kriegstein AR. Neurons derived from radial glial cells establish radial units in neocortex. Nature. 2001; 409:714–720. [PubMed: 11217860]

Noctor SC, Flint AC, Weissman TA, Wong WS, Clinton BK, Kriegstein AR. Dividing precursor cells of the embryonic cortical ventricular zone have morphological and molecular characteristics of radial glia. J Neurosci. 2002; 22:3161–3173. [PubMed: 11943818]

Okumura A, Hayakawa F, Kato T, Kuno K, Watanabe K. MRI findings in patients with spastic cerebral palsy. I: correlation with gestational age at birth. Dev Med Child Neurol. 1997; 39:363–368. [PubMed: 9233359]

Olney JW, Ikonomidou C, Mosinger JL, Freidich G. MK-801 prevents hypobaric/ischemic neuronal damage in infant rat brain. J Neurosci. 1989; 9:1701–1704. [PubMed: 2656934]

Ong WY, Leong SK, Garey LJ, Reynolds R. A light- and electron-microscopic study of GluR4-positive cells in cerebral cortex, subcortical white matter and corpus callosum of neonatal, immature and adult rats. Exp Brain Res. 1996; 110:367–378. [PubMed: 8871096]

Owens J, Robbins CA, Wenzel J, Schwartzkroin PA. Acute and chronic effects of hypoxia on the developing hippocampus. Ann Neurol. 1997; 41:187–199. [PubMed: 9029068]

Patneau DK, Wright PW, Wisden W. Glial cells of the oligodendrocyte lineage express both kainate- and AM PA-preferring subtypes of glutamate receptor. Neuron. 1994; 12:357–371. [PubMed: 7509160]

Pellegrini-Giampietro DE, Bennett MVL, Zukin RS. Differential expression of three glutamate receptor genes in developing rat brain: an in situ hybridization study. Proc Natl Acad Sci U S A. 1991; 88:4157–4161. [PubMed: 1851996]

Pellegrini-Giampietro DE, Bennett MVL, Zukin RS. Are Ca^{2+}-permeable kainate/AMPA receptors more abundant in immature brain? Neurosci Lett. 1992; 144:65–69. [PubMed: 1331916]

Petralia RS, Wenthold RJ. Light and electron immunocytochemical localization of AMP A-selective glutamate receptors in the rat brain. J Comp Neurol. 1992; 318:329–354. [PubMed: 1374769]

Petralia RS, Yokotani N, Wenthold RJ. Light and electron microscope distribution of the NMDA receptor subunit NMDAR1 in the rat nervous system using a selective anti-peptide antibody. J Neurosci. 1994; 14:667–696. [PubMed: 8301357]

Petralia RS, Wang Y-X, Mayat E, Wenthold RJ. Glutamate receptor subunit 2-selective antibody shows a differential distribution of calcium-impermeable AMPA receptors among populations of neurons. J Comp Neurol. 1997; 385:456–476. [PubMed: 9300771]

Renart J, Sandoval IV. Western blots. Methods Enzymol. 1984; 104:455–460. [PubMed: 6717294]

Roland EH, Poskitt K, Rodriguez E, Lupton BA, Hill A. Perinatal hypoxic-ischemic thalamic injury: clinical features and neuroimaging. Ann Neurol. 1998; 44:161–166. [PubMed: 9708537]

Rosenberg PA, Dai W, Gan XD, Ali S, Fu J, Back SA, Sanchez RM, Segal MM, Follett PL, Jensen FE, Volpe JJ. Mature myelin basic protein-expressing oligodendrocytes are insensitive to kainate toxicity. J Neurosci Res. 2003; 71:237–245. [PubMed: 12503086]

Saliba RM, Annegers JF, Waller DK, Tyson JE, Mizrahi EM. Incidence of neonatal seizures in Harris County, Texas, 1992–1994. Am J Epidemiol. 1999; 150:763–769. [PubMed: 10512430]

Sanchez RM, Koh S, Rio C, Wang C, Lamperti ED, Sharma D, Corfas G, Jensen FE. Decreased glutamate receptor 2 expression and enhanced epileptogenesis in immature rat hippocampus after perinatal hypoxia-induced seizures. J Neurosci. 2001; 21:8154–8163. [PubMed: 11588188]

Sanchez RM, Dai W, Levada RE, Lippman JJ, Jensen FE. AMPA/kainate receptor-mediated down-regulation of GABAergic synaptic transmission by calcineurin after seizures in the developing rat brain. J Neurosci. 2005; 25:3442–3451. [PubMed: 15800199]

Schipke CG, Ohlemeyer C, Matyash M, Nolte C, Kettenmann H, Kirchhoff F. Astrocytes of the mouse neocortex express functional N-methyl-D-aspartate receptors. FASEB J. 2001; 15:1270–1272. [PubMed: 11344110]

Seeburg PH. The TIPS/TINS Lecture: the molecular biology of the mammalian glutamate receptor channels. Trends Neurosci. 1993; 14:297–303.

Seifert G, Steinhauser C. Glial cells in the mouse hippocampus express AMPA receptors with an intermediate Ca^{2+} permeability. Eur J Neurosci. 1995; 7:1872–1881. [PubMed: 8528461]

Seifert G, Zhou M, Steinhauser C. Analysis of AMPA receptor properties during postnatal development of mouse hippocampal astrocytes. J Neurophysiol. 1997; 78:2916–2923. [PubMed: 9405512]

Sheldon RA, Chuai J, Ferriero DM. A rat model for hypoxic-ischemic brain damage in very premature infants. Biol Neonate. 1996; 69:327–341. [PubMed: 8790911]

Shelton MK, McCarthy KD. Mature hippocampal astrocytes exhibit functional metabotropic and ionotropic glutamate receptors in situ. Glia. 1999; 26:1–11. [PubMed: 10088667]

Silverstein FS, Naik B, Simpson J. Hypoxia-ischemia stimulates hippocampal glutamate efflux in perinatal rat brain: an in vivo micro-dialysis study. Pediatr Res. 1991; 30:587–590. [PubMed: 1687160]

Stichel CC, Muller CM, Zilles K. Distribution of glial fibrillary acidic protein and vimentin immunoreactivity during rat visual cortex development. J Neurocytol. 1991; 20:97–108. [PubMed: 2027041]

Super H, Del Rio JA, Martinez A, Perez-Sust P, Soriano E. Disruption of neuronal migration and radial glia in the developing cerebral cortex following ablation of Cajal-Retzius cells. Cereb Cortex. 2000; 10:602–613. [PubMed: 10859138]

Takahashi T, Misson JP, Caviness VS Jr. Glial process elongation and branching in the developing murine neocortex: a qualitative and quantitative immunohistochemical analysis. J Comp Neurol. 1990; 302:15–28. [PubMed: 2086612]

Talos DM, Follett PL, Folkerth RD, Fishman RE, Trachtenberg FL, Volpe JJ, Jensen FE. Developmental regulation of AMPA receptor subunit expression in forebrain and relationship to regional susceptibility to hypoxic/ischemic injury: part II. Human cerebral white matter and cortex. J Comp Neurol. 2006; 497:61–77. [PubMed: 16680761]

Tamamaki N, Nakamura K, Okamoto K, Kaneko T. Radial glia is a progenitor of neocortical neurons in the developing cerebral cortex. Neurosci Res. 2001; 41:51–60. [PubMed: 11535293]

Towfighi J, Mauger D, Vannucci RC, Vannucci SJ. Influence of age on the cerebral lesions in an immature rat model of cerebral hypoxia-ischemia: a light microscopic study. Brain Res Dev Brain Res. 1997; 100:149–160.

Volpe, JJ. Neurology of the newborn. Philadelphia: Saunders; 2001.

Washburn MS, Numberger M, Zhang S, Dingledine R. Differential dependence on GluR2 expression of three characteristic features of AMPA receptors. J Neurosci. 1997; 17:9393–9406. [PubMed: 9390995]

Wenthold RJ, Yokotani N, Doi K, Wada K. Immunochemical characterization of the non-NMDA glutamate receptor using subunit-specific antibodies. J Biol Chem. 1992; 267:501–507. [PubMed: 1309749]

Yamaya Y, Yoshioka A, Saiki S, Yuki N, Hirose G, Pleasure D. Type-2 astrocyte-like cells are more resistant than oligodendrocyte-like cells against non-N-methyl-D-aspartate glutamate receptor-mediated exci to toxicity. J Neurosci Res. 2002; 70:588–598. [PubMed: 12404513]

Yuan X, Eisen AM, McBain CJ, Gallo V. A role for glutamate and its receptors in the regulation of oligodendrocyte development in cerebellar tissue slices. Development. 1998; 125:2901–2914. [PubMed: 9655812]

Zhou CJ, Zhao C, Pleasure SJ. Wnt signaling mutants have decreased dentate granule cell production and radial glial scaffolding abnormalities. J Neurosci. 2004; 24:121–126. [PubMed: 14715945]

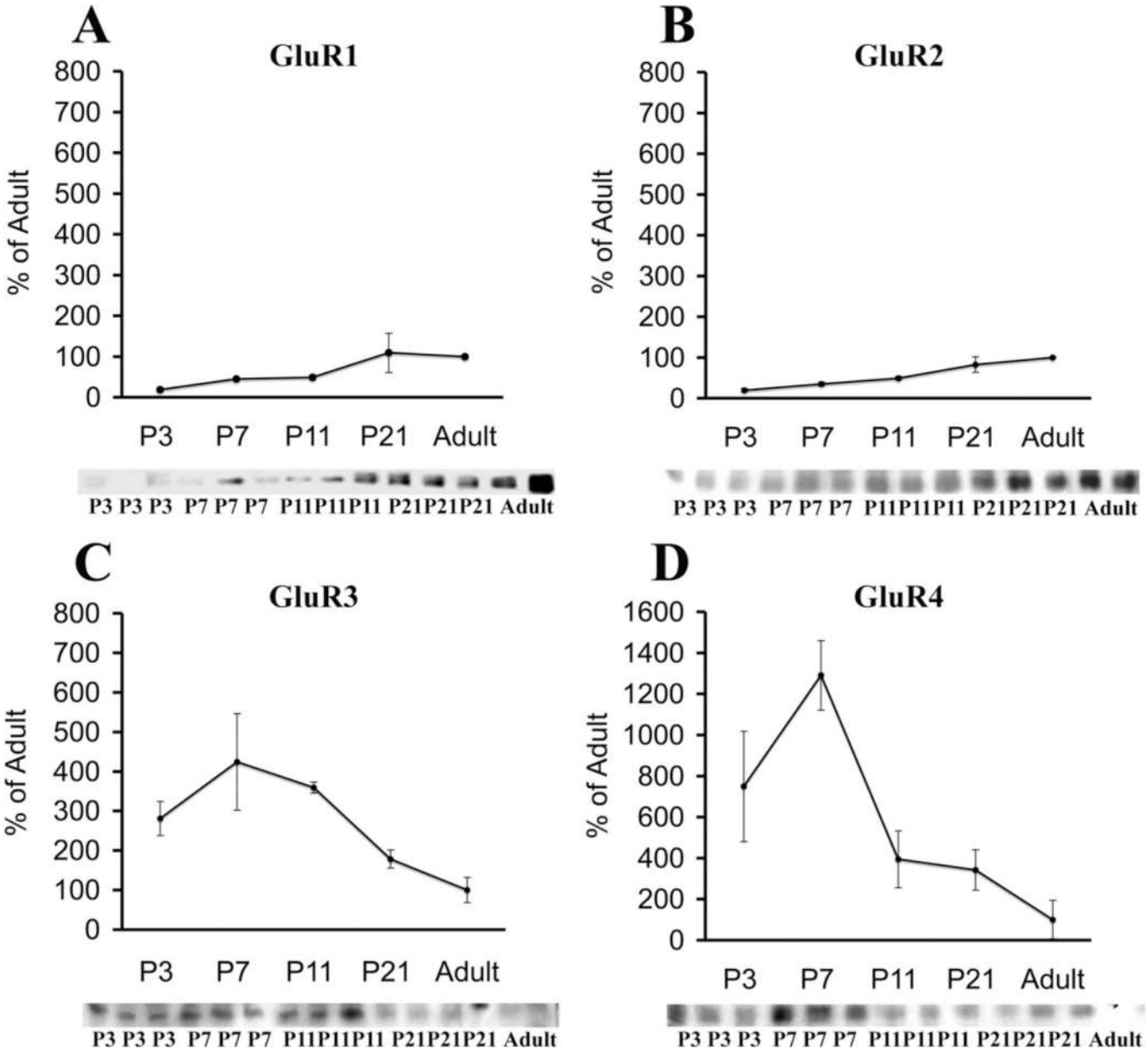

Fig. 1.

Developmental regulation of membrane-expressed AMPAR subunits in the white matter from Long Evans rats. Western blot quantification of GluR1–GluR4 subunits in the rat white matter at different postnatal ages, compared with adult standard (100/%), demonstrates that, at P7, GluR1 (**A**) and GluR2 (**B**) subunits are expressed at lower-than-adult levels, whereas GluR3 (**C**) and GluR4 (**D**) expression is significantly up-regulated. **Insets** are corresponding Western blots.

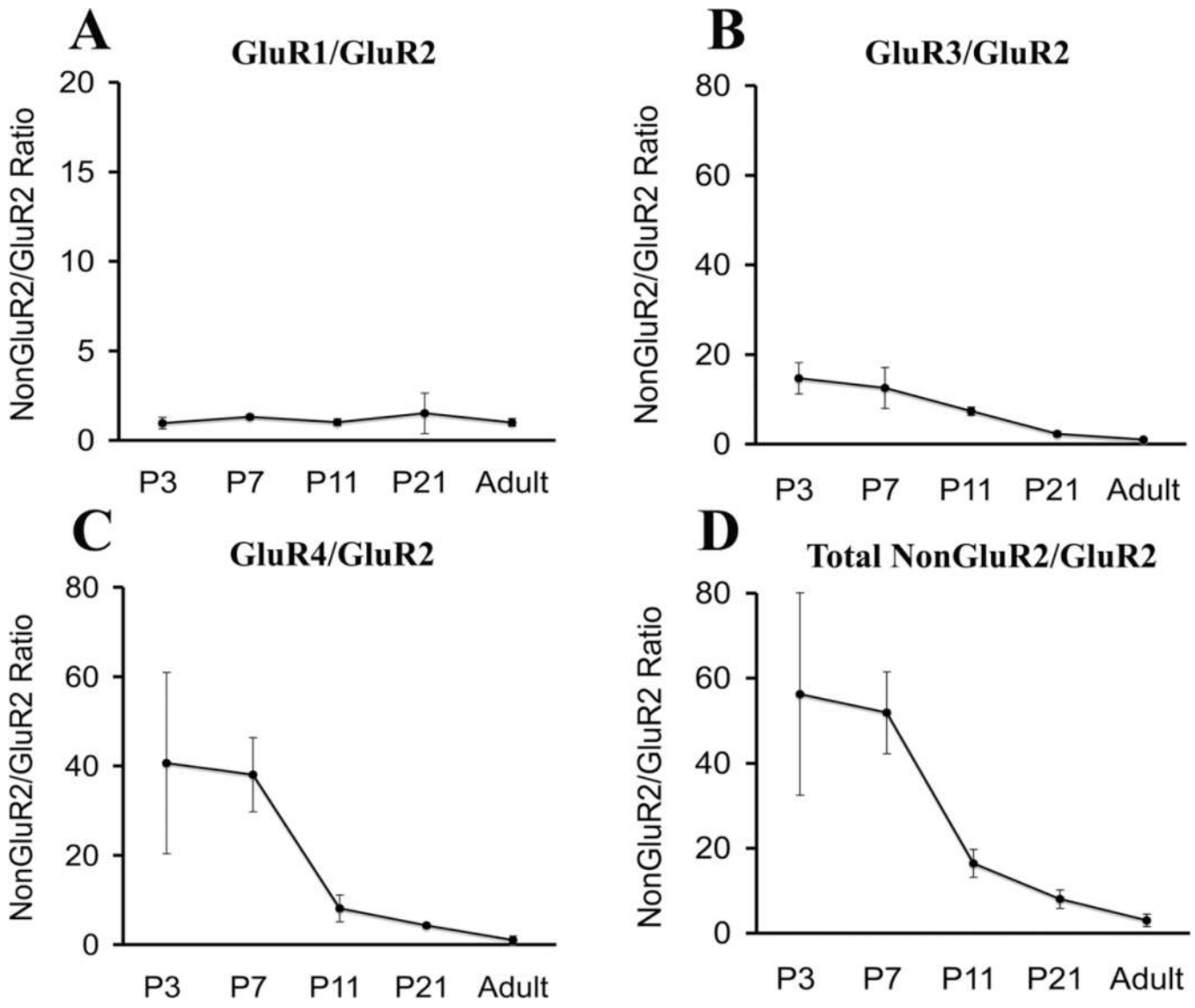

Fig. 2.

Non-GluR2/GluR2 ratios in the white matter from Long Evans rats, expressed as a function of postnatal age. GluR1/GluR2 ratio (**A**) shows no significant variation with age, whereas GluR3/GluR2 (**B**), GluR4/GluR2 (**C**), and total nonGluR2/GluR2 ratios (**D**) are significantly higher at P3 and P7, relative to adult.

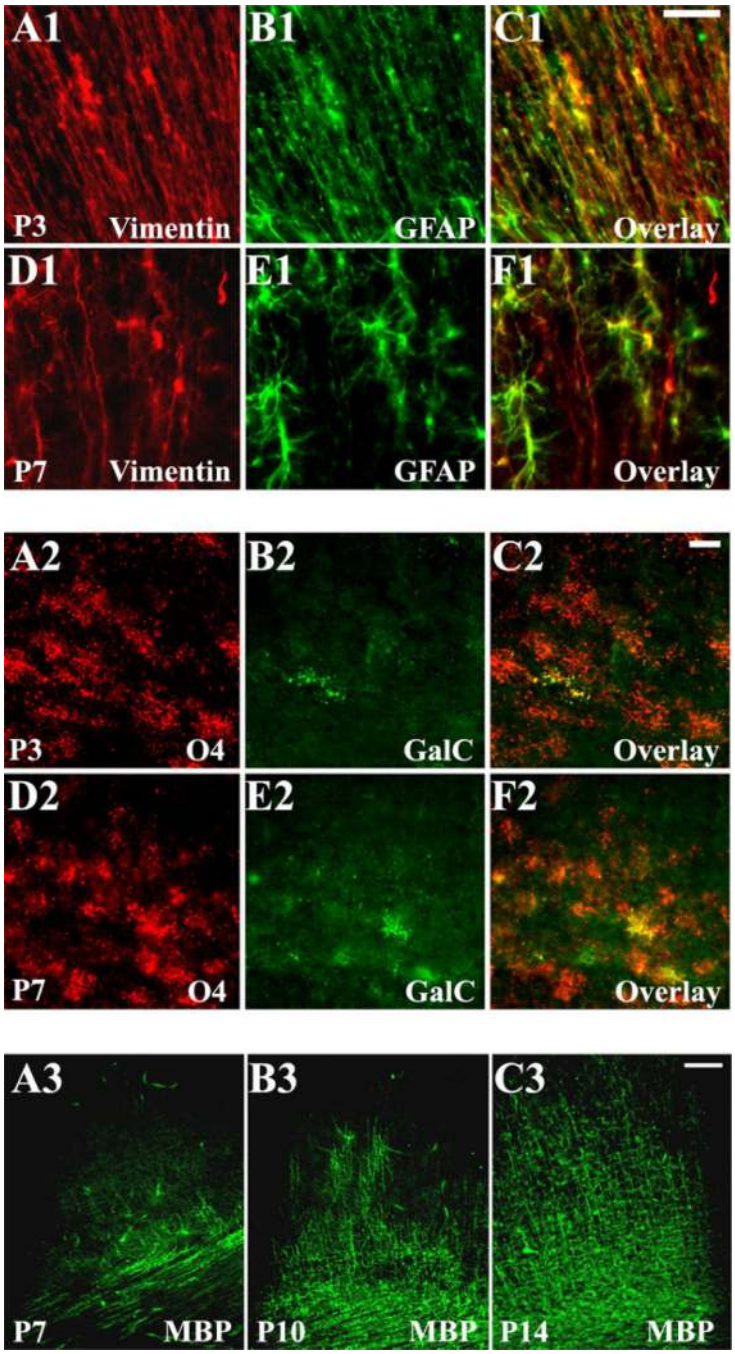

Fig. 3.

White matter cellular development in Long Evans rats, assessed by atroglial and oligodendroglial stage-specific markers. Developing astroglia (A1–F1) is represented mainly by vimentin^{+}/GFAP^{+} radial glia at P3 (**A1–C1**); at P7 (**D1–F1**) vimentin^{-}/GFAP^{+} mature astrocytes predominate. Developing oligodendroglia (A2–F2) is represented predominantly by 04^{+}/GalC^{-} OL precursors at P3 (**A2–C2**) and by 04^{+}/GalC^{+} immature OLs at P7 (**D2–F2**). MBP-expressing mature OLs represent only a minor population at P7 (**A3**), but their number increase progressively with age, as seen at P10 (B3) and P14 (**C3**). Scale bars = 20

μm in C1 (applies to A1–F1); 10 μm in C2 (applies to A2–F2); 50 μm in C3 (applies to A3–C3).

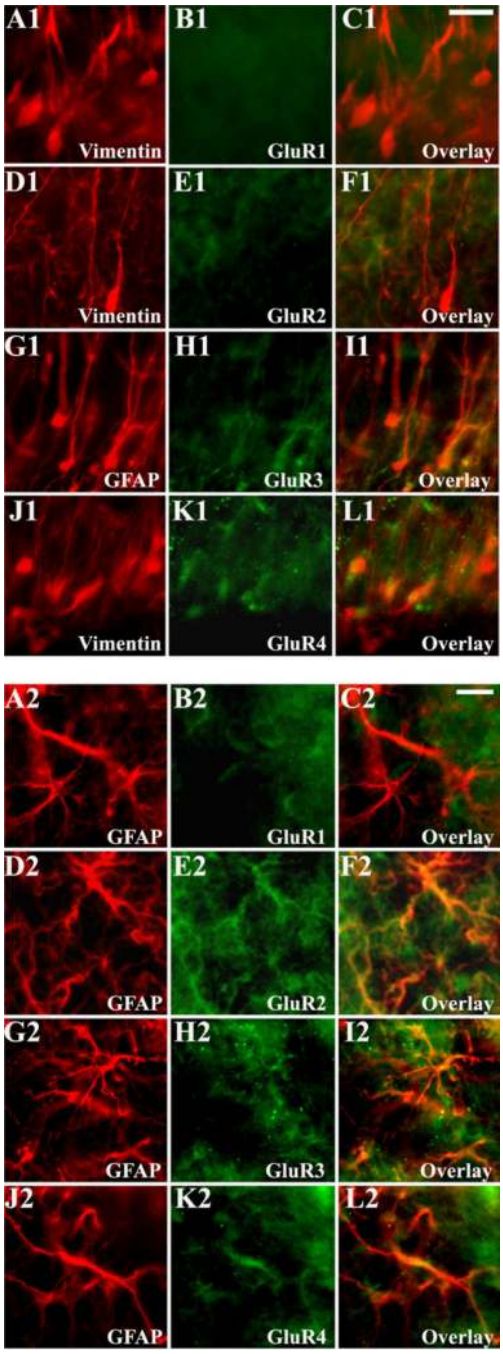

Fig. 4.

Maturational profile of AMPAR subunit expression on developing astroglia from Long Evans rats. Radial glia is the first cell type to express AMPAR subunits (A1–L1). At P3, radial glia cell bodies and proximal processes, labeled with vimentin (Al–Fl and J1–L1) and GFAP (G1–I1), are intensely GluR3 (**G1–I1**) and GluR4 (**J1–L1**) positive, whereas GluR1 (**A1–C1**) and GluR2 (**D1–F1**) levels are low. At P11, GFAP^{+} astrocytes (A2–L2) express increased GluR2 (**D2–F2**), GluR3 (**G2–I2**), and GluR4 (**J2–L2**), whereas intense GluR1 expression in the subcortical white matter is observed exclusively in nonastrocytic cellular

elements (**A2–C2**). Scale bars = 10 μm in C1 (applies to A1–L1); 10 μm in C2 (applies to A2–L2).

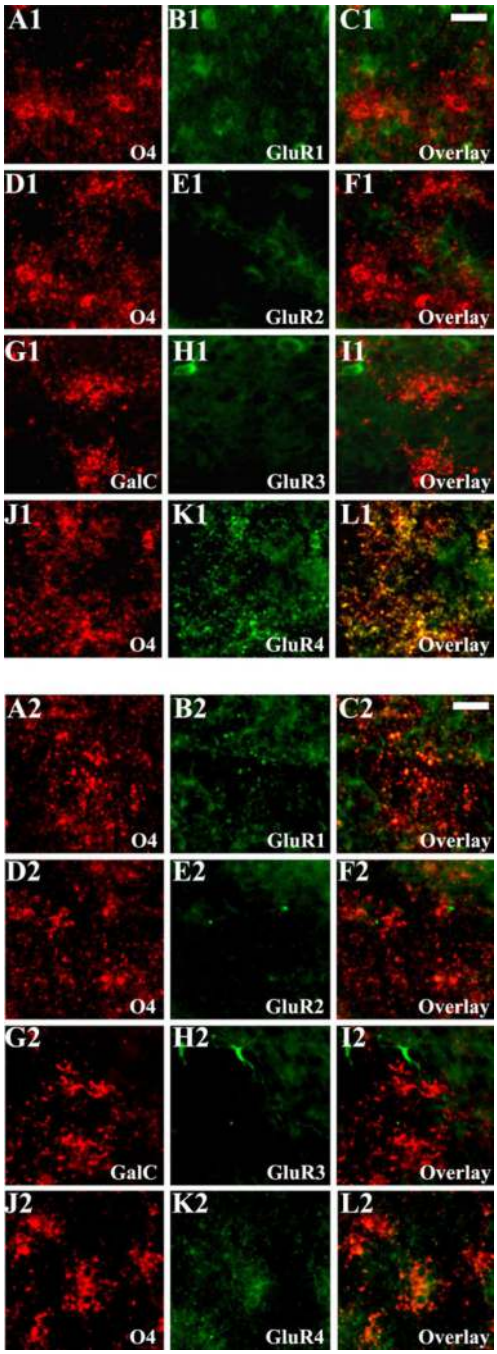

Fig. 5.

Differential AMPAR subunit expression on white matter pre-oligodendrocytes from Long Evans rats. At P7 (A1–L1), during the time of peak expression, immunocytochemical analysis of the $O4^+$ (A1–F1 and J1–L1) or$GalC^+$ (G1–I1) pre-OLs demonstrates increased GluR4 immunoreactivity on both cell bodies and processes (J1–L1), in contrast to a relative lack in GluR1 (**A1–C1**), GluR2 (**D1–F1**), and GluR3 (**G1–I1**). At P11 (A2–L2), AMPAR expression on $O4^+$ (A2–F2 and J2–L2) or $GalC^+$(**G2–I2**) pre-OLs demonstrates that GluR4 immunoreactivity is substantially diminished (**J2–L2**), although the relative GluR1 (**A2–**

C2), GluR2 (**D2–F2**), and GluR3 (**G2–I2**) deficiency persists at this age. Scale bars = 10 μm in C1 (applies to A1–L1); 10 μm in C2 (applies to A2–L2).

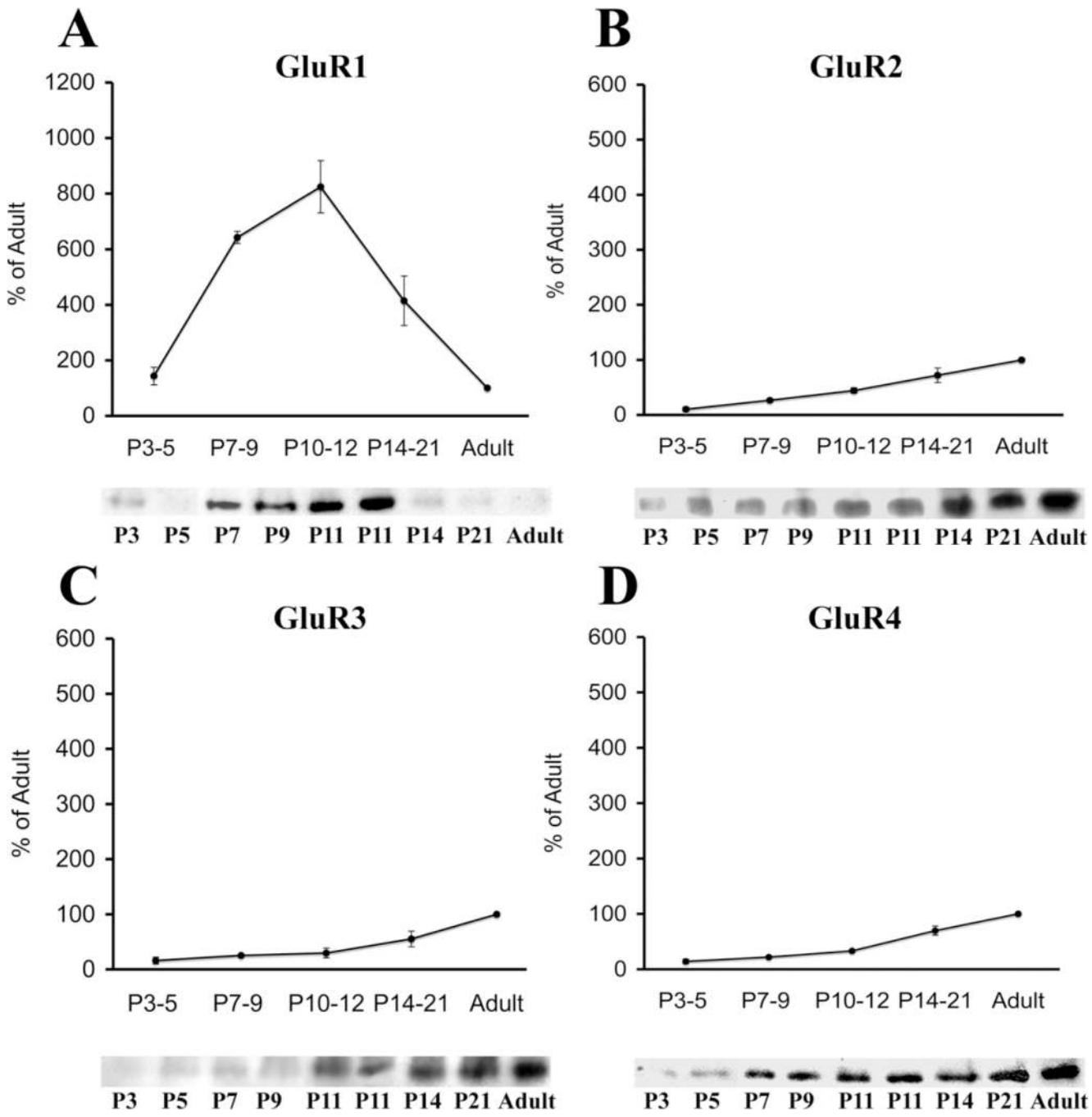

Fig. 6.

Developmental regulation of AMPAR subunits in cortical membrane fractions from Long Evans rats. Western blot analysis of AMPAR subunits during the first 3 postnatal weeks demonstrates that, relative to adult levels (100%), GluR1 (**A**) expression levels are significantly increased between P7 and P14, whereas, at the same age, GluR2 (**B**), GluR3 (**C**), and GluR4 (**D**) expression remains below adult levels. **Insets** are representative Western blots.

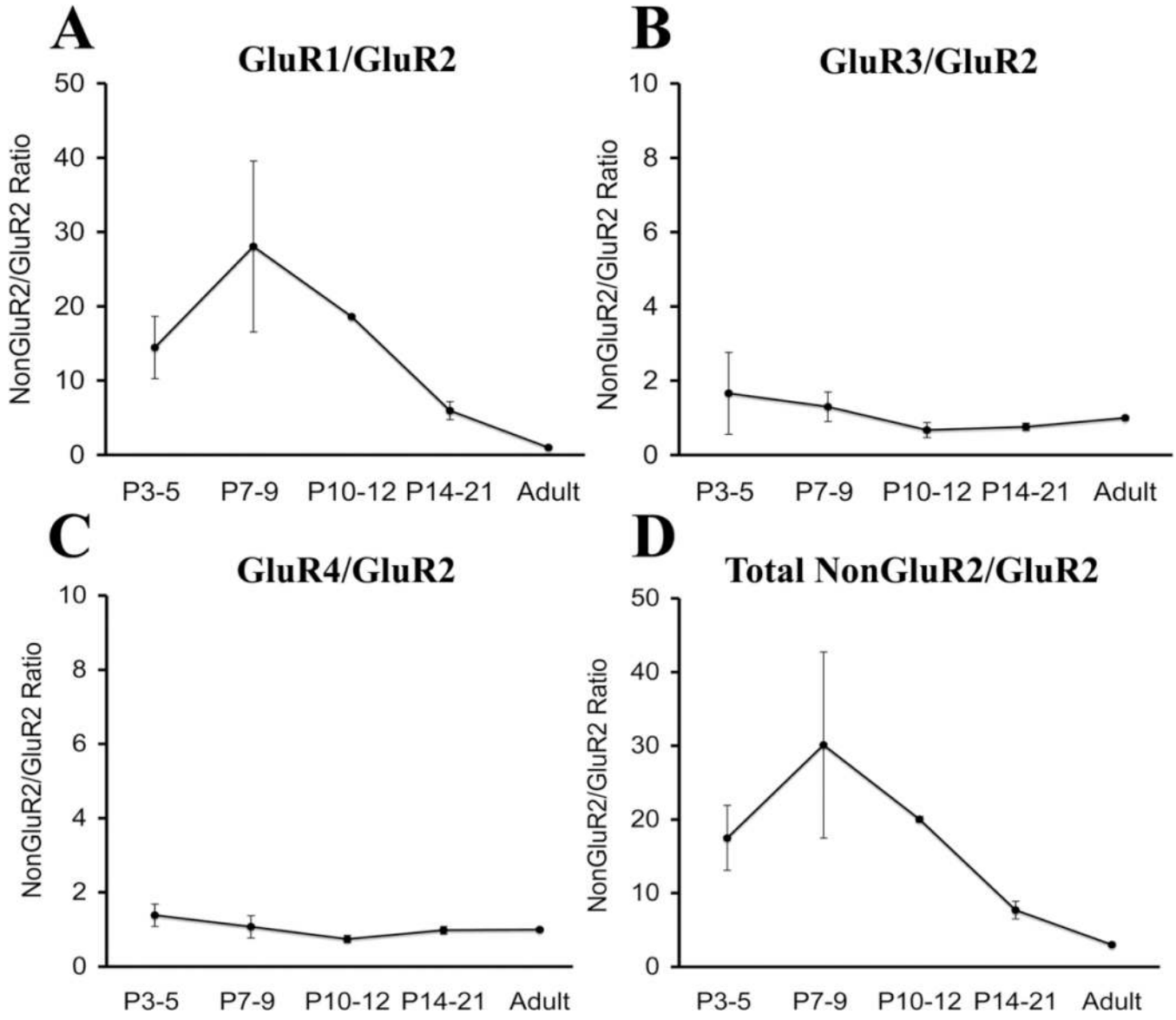

Fig. 7.

Non-GluR2/GluR2 ratios in the cortex from Long Evans rats, expressed as a function of postnatal age. GluR1/GluR2 (**A**) and total nonGluR2/GluR2 (**D**) ratios are significantly higher at younger ages relative to adult, peaking at P7–P9. By contrast, during the entire developmental window analyzed, GluR3/GluR2 (**B**) and GluR4/GluR2 (**C**) are low and comparable to adult values.

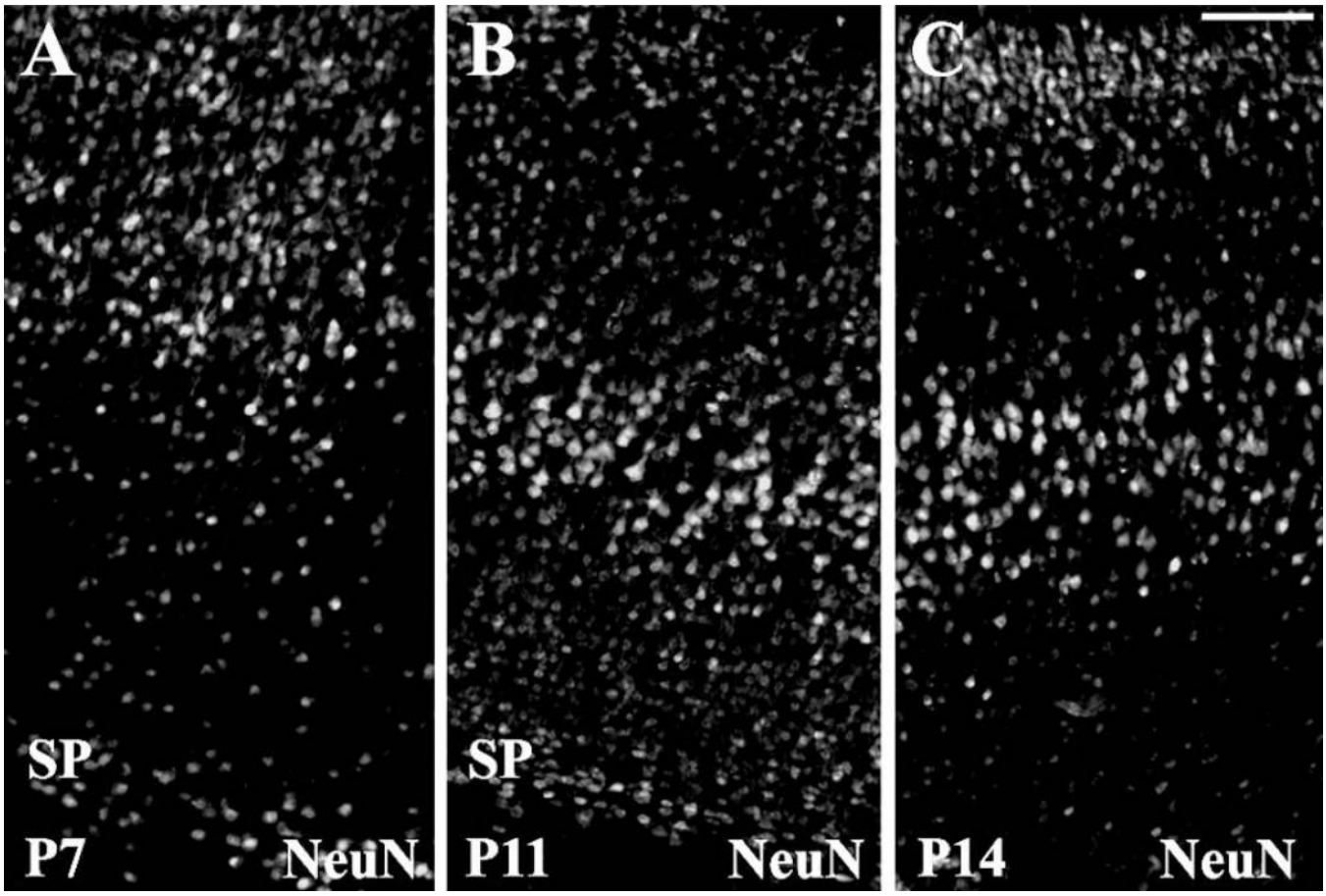

Fig. 8.

Layer-specific cortical maturational changes in Long Evans rats, assessed by NeuN immunoreactivity. At P7 (**A**), the developing cortex is characterized by the presence of a thick subcortical plate (SP) located beneath the cortical plate. At P11 (**B**), the subplate slightly diminishes, and, in the overlying cortex, all layers are visible. At P14 (**C**), the subplate region is indistinguishable from the cortex, which increases significantly in thickness. Scale bar = 50 μm.

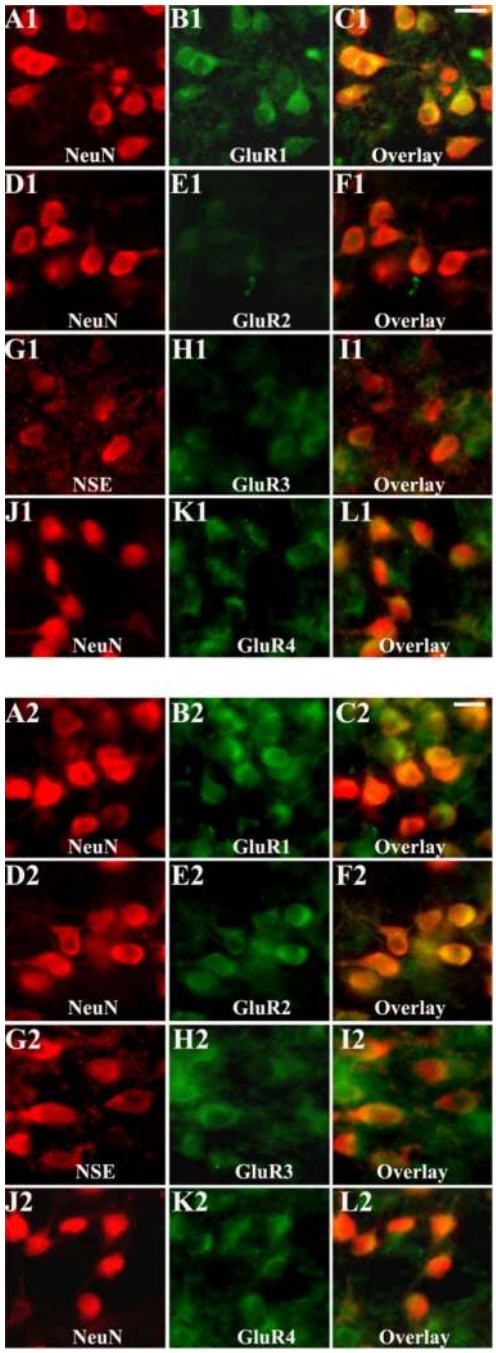

Fig. 9.

Expression profile of AMPAR subunits on the subplate neurons in Long Evans rats during early postnatal development. At P7 (A1–L1), coronal sections double labeled with NeuN (A1–F1 and J1–L1) and neuron-specific enolase (NSE; G1–I1) show subcortical neurons strongly labeled with GluR1 (**A1–C1**) and GluR4 (**J1–L1**) but only to a very minimal extent with GluR2 (**D1–F1**) and GluR3 (**G1–I1**). In contrast, at P11 (A2–L2), double labeling with NeuN (A2–F2 and J2–L2) and NSE (G2–I2) demonstrates that, although the GluR1 (**A2–C2**) and GluR4 (**J2–L2**) staining pattern remains unchanged, subplate neurons display

intense GluR2 (**D2–F2**) and GluR3 (**G2–I2**) immunoreactivity. Scale bars = 10 μm in C1 (applies to A1–L1); 10 μm in C2 (applies to A2–L2).

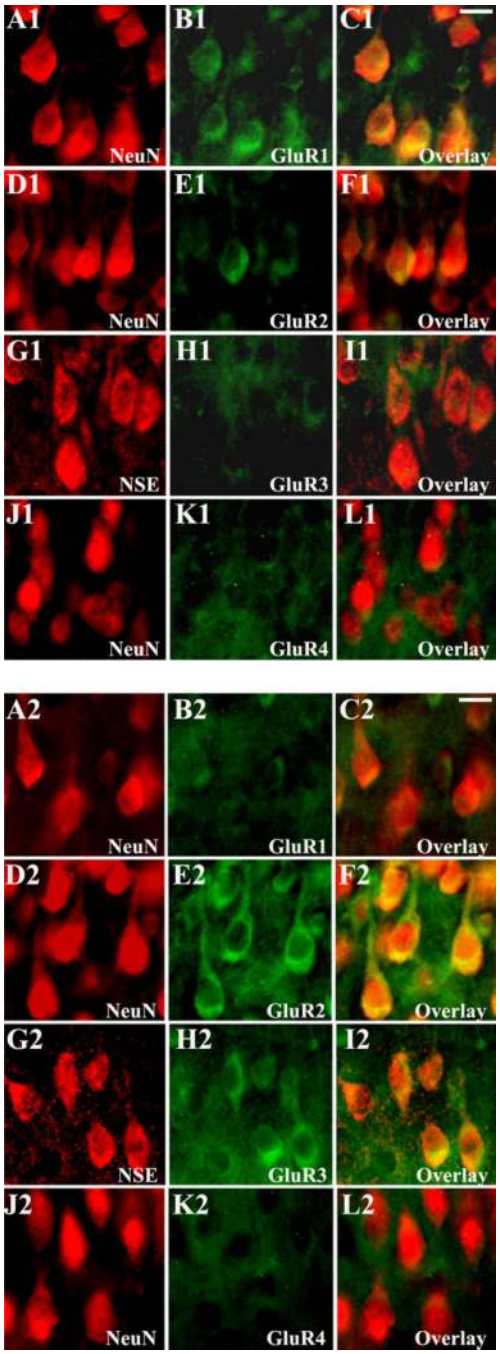

Fig. 10.

Age-specific changes in AMPAR subunit expression on layer V cortical pyramidal neurons in Long Evans rats during the second and third postnatal weeks. At P11 (A1–L1), cortical pyramidal neurons, labeled with NeuN (A1–F1 and J1–L1) and NSE (G1–I1), express high GluR1 levels (**A1–C1**), in contrast to minimal GluR2 (**D1–F1**), GluR3 (**G1–I1**), and GluR4 (**J1–L1**) expression. At P18 (A2–L2), immunostaining with NeuN (A2–F2 and J2–L2) and NSE (G2–I2) in combination with AMPAR subunits demonstrates that pyramidal neuron GluR1 expression (**A2–C2**) is substantially less than at P11 (A1–C1), although both GluR2

(**D2–F2**) and GluR3 (**G2–I2**) expressions are now much more robust relative to P11 (D1–I1). GluR4 levels (**J2–L2**) remain in contrast constantly low. Scale bars = 10 μm in C1 (applies to A1–L1); 10 μm in C2 (applies to A2–L2).

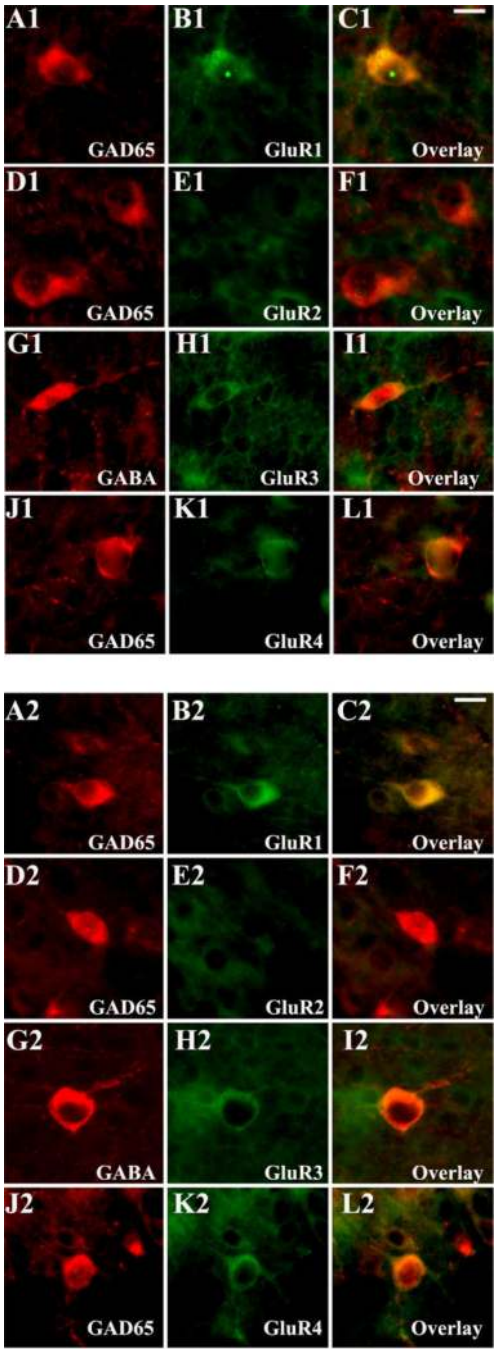

Fig. 11.

Distinct postnatal developmental regulation of GluR1– GluR4 AMPAR subunits in layer VI cortical nonpyramidal neurons from Long Evans rats. At P10 (A1–L1), nonpyramidal neurons, labeled with GAD-65 (A1–F1 and J1–L1) and GABA (G1-I1), demonstrate GluR1 (**A1–C1**), GluR3 (**G1–I1**), and GluR4 (**J1–L1**) labeling on both cell bodies and processes, in contrast to a relative lack of GluR2 (**D1–F1**) immunoreactivity. At P21 (A2–L2), GAD–65 (A2–F2 and J2–L2)- and GABA (G2–I2)-immunopositive nonpyramidal neurons show an increased GluR1 (**A2–C2**), GluR3 (**G2–I2**), and GluR4 (**J2–L2**) expression, without a

significant change in GluR2 (**D2–F2**) staining. Scale bars = 10 μm in C1 (applies to A1–L1); 10 μm in C2 (applies to A2–L2).

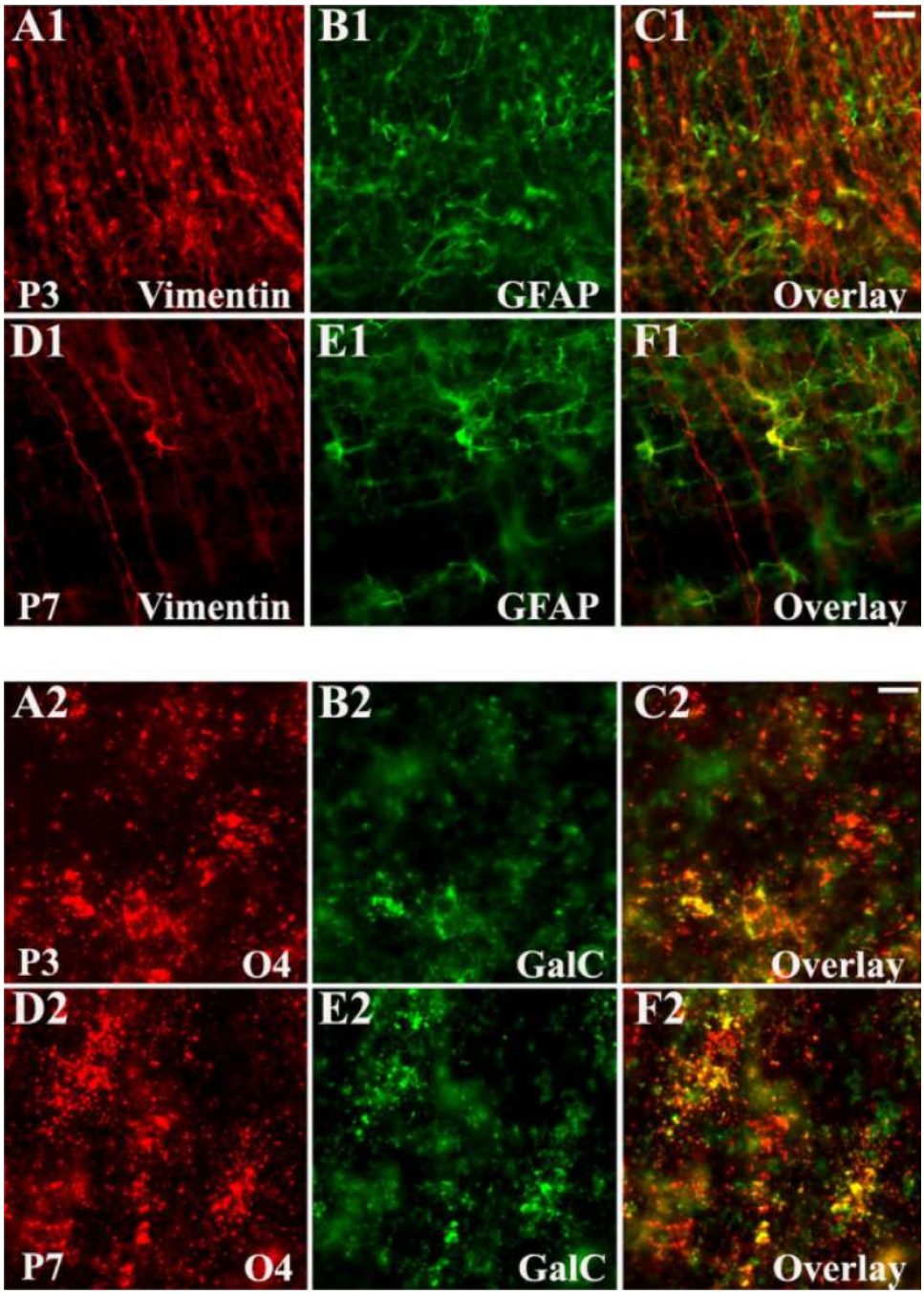

Fig. 12.

Astroglial and oligodendroglial lineage maturation in Sprague Dawley rats revealed by differential expression of stage-specific markers. Vimentin^{-}/GFAP^{+} astrocytes are abundant at P3 (**A1–C1**) and predominate at P7 (**D1–F1**). Similarly, O4^{+}/GalC^{+} pre-OLs are numerous at P3 (**A2–C2**), increasing at P7 (**D2–F2**). Scale bars = 20 μm in C1 (applies to A1–F1); 10 μm in C2 (applies to A2–F2).

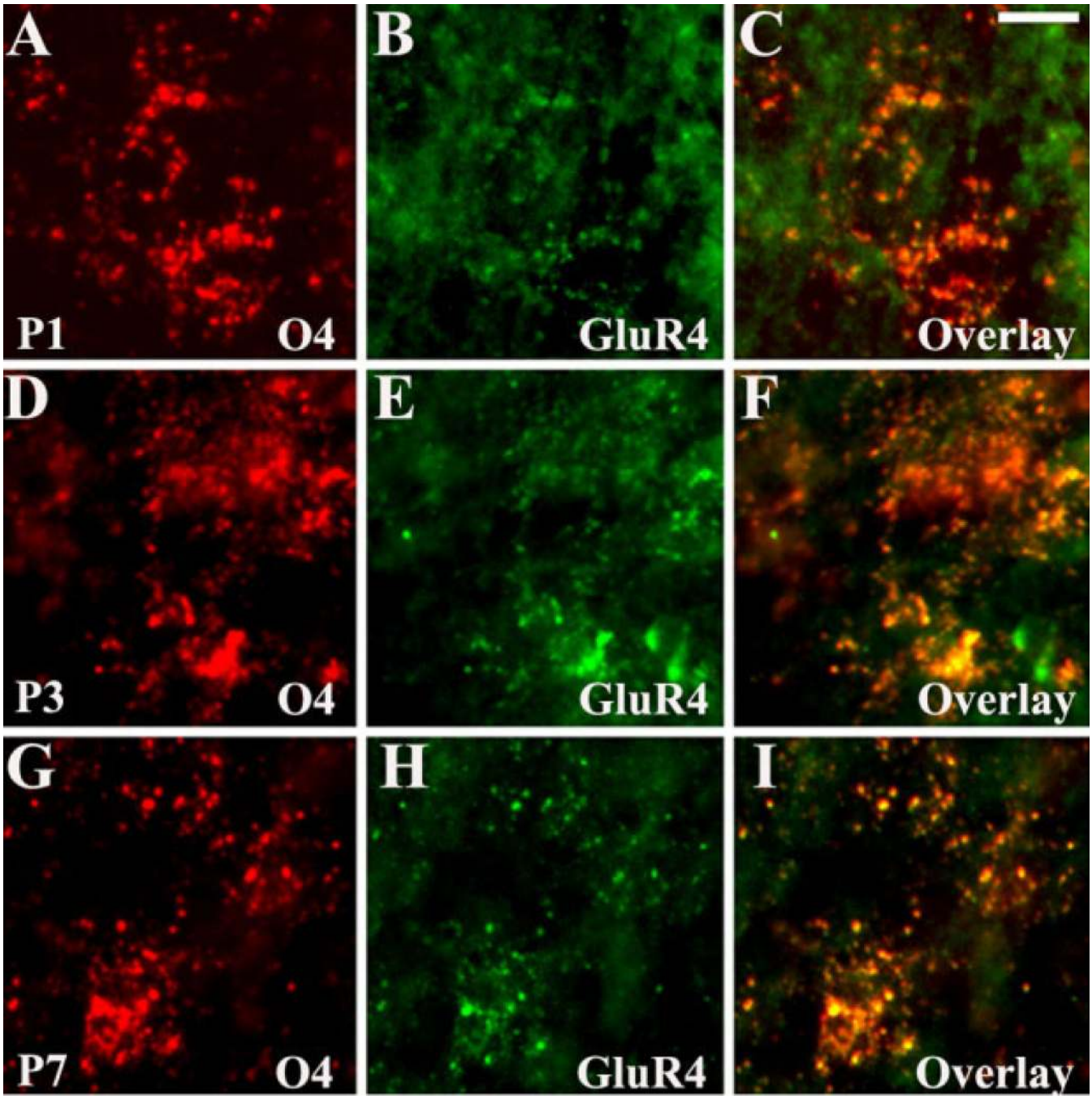

Fig. 13.

Specific regulation of GluR4 subunit on $O4^+$ pre-OLs in Sprague Dawley rats. White matter pre-OLs display minimal GluR4 expression at P1 (**A–C**) but show robust GluR4 staining at P3 (**D–F**) and P7 (**G–I**). Scale bar = 10 μm.

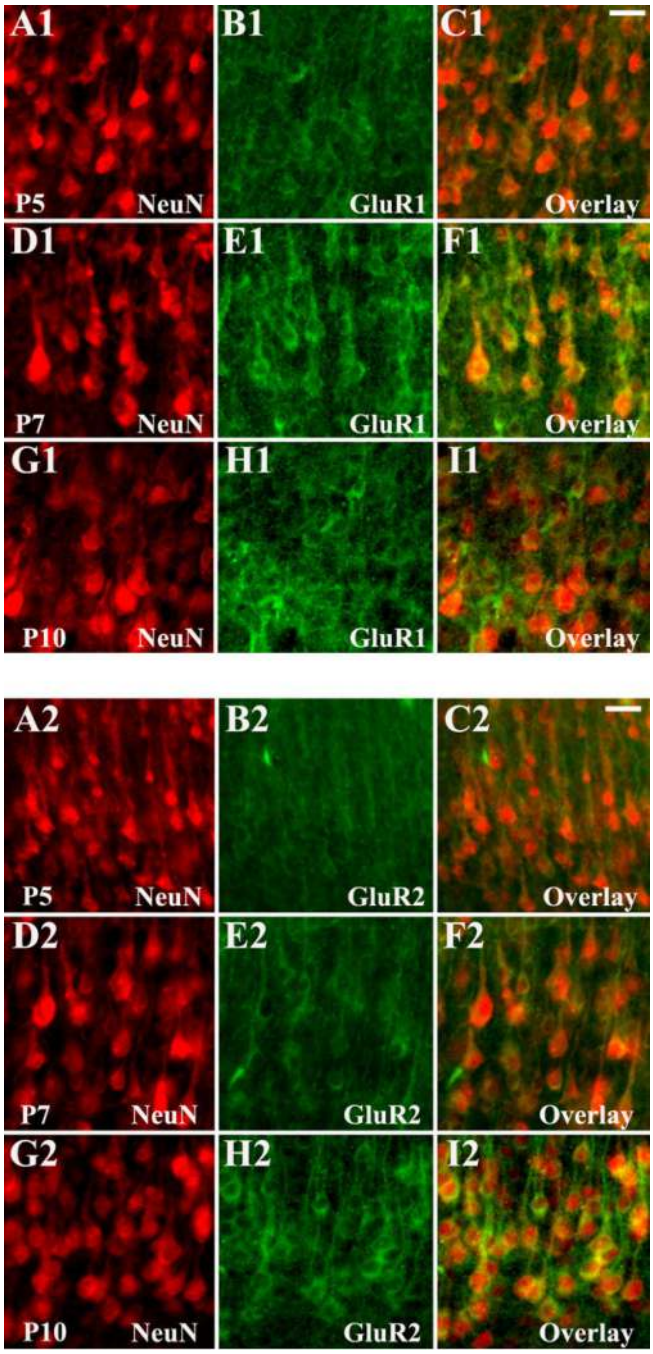

Fig. 14.

Differential regulation of AMPAR subunits GluR1 (A1–I1) and GluR2 (A2–I2) on cortical neurons in Sprague Dawley rats. GluR1 subunit expression (A1–I1) is highest on pyramidal and nonpyramidal neurons at P7 (**D1–F1**), compared with P5 (**A1–C1**) and P10 (**G1–I1**). GluR2 expression (A2–I2) remains low at P5 (**A2–C2**) and **P7** (**D2–F2**) and increases substantially on pyramidal neurons at P10 (**G2–I2**). Scale bars = 20 μm in C1 (applies to A1–I1); 20 μm in C2 (applies to A2–I2).

TABLE 1

Antibodies Used for Single- and Double-Label Immunocytochemistry and Western Blot (WB)[1]

Antibody	Source	Host and type	Antigen	Specificity[2]	Dilution
GluR1 (AB 1504)	Chemicon International, Temecula, CA	Rabbit poly-IgG	C-terminus peptide (aa.877–889) of rat GluR1 (-SHSSGMPLGATGL-)	Detects 1 band at 108 kDa on Western blot of rat brain homogenates (1)	1:200, 1:100–1:200 (WB)
GluR2 (AB 1768)	Chemicon International	Rabbit poly-IgG	Peptide near C-terminus (aa.827–842) of rat GluR2 (-VAKNPQNINPSSSQNS-)	Detects a single band at 108 kDa on immunoblot of rat brain tissues (2)	1:200, 1:100–1:200 (WB)
GluR3 (MAB 5416)	Chemicon International	Mouse mono-IgG	Fusion protein containing residues 245–451 from the N-terminal of GluR3	Detects 1 band at ~110 kDa on Western blot of rat brain homogenates (3)	1:400, 1:250–1:500 (WB)
GluR4 (AB 1508)	Chemicon International	Rabbit poly-IgG	C-terminal peptide (aa.868–881) of rat GluR4 (-RQSSGLAVIASDLP-)	Recognizes 1 band at 108 kDa on Western blot of rat brain homogenates (1)	1:100, 1:50–1:100 (WB)
Vimentin (MAB 3400)	Chemicon International	Mouse mono-IgG	Purified porcine vimentin	Detects a 57-kDa band specific for vimentin on immunoblots of human glioma cell lines (4)	1:500
GFAP (SMI 22)	Sternberger Monoclonals, Lutherville, MD	Mouse mono-IgG (mixture)	Purified bovine GFAP	All components (clones 1B4, 2E1, 4A11) are specific for GFAP by radioimmunoassay, Western blot, and immunocytochemistry (5)	1:1,000
GFAP (AB 5804)	Chemicon International	Rabbit poly-IgG	Purified bovine GFAP	Largely colocalizes with monoclonal GFAP (6)	1:500
O1	Gift from Dr S. Pfeiffer, Farmington, CT	Mouse mono-IgM	Bovine corpus callosum (7)	Recognizes specifically GalC and MG expressed on OL surface on lipid immunodot blots (8)	1:500
O4	Gift from Dr. S. Pfeiffer	Mouse mono-IgM	Bovine corpus callosum (7)	Reacts selectively with OL surface antigens sulfatide and seminolipid on lipid immunodot blots (8)	1:500
GalC (AB 142)	Chemicon International	Rabbit poly-IgG	Purified bovine GalC	Colocalizes with monoclonal O1 (6)	1:100
MBP (SMI 99)	Sternberger Monoclonals	Mouse mono-IgG	Human MBP peptide containing aa 131–136 (-Ala-Ser-Asp-Tyr-Lys-Ser-)	Detects 4 bands between 14 and 21 kDa, corresponding to 4 MBP isoforms on immunoblots of rat cerebellum (9)	1:1,000
NeuN (MAB 377)	Chemicon International	Mouse mono-IgG	Purified cell nuclei from mouse brain	Recognizes 2 bands on Western blot of mouse brain, corresponding to the 46- and 48-kDa NeuN isoforms (10)	1:100
NSE (AB 951)	Chemicon International	Rabbit poly-IgG	Synthetic peptide from human	Detects a single band at 39 kDa	1:200

J Comp Neurol. Author manuscript; available in PMC 2015 February 02.

Antibody	Source	Host and type	Antigen	Specificity[2]	Dilution
			NSE	on Western blots of purified bovine NSE (11)	
GAD-65 (MAB 351)	Chemicon International	Mouse mono-IgG	Purified rat GAD	Detects a 59-kDa band, corresponding to the 65 kDa GAD isoform on Western blot of whole rat brain (12)	1:1,000
GABA (A-2052)	Sigma, St. Louis, MO	Rabbit poly-IgG	BSA-conjugated GABA	Shows positive binding with GABA, but not BSA in dot blot assay (13)	1:1,000

[1]Poly, polyclonal; mono, monoclonal; aa, aminoacids; GFAP, glial fibrillary acidic protein; O4, O1, OL progenitor surface markers; GalC, galactocerebroside; MG, monogalactosyl-digliceride; MBP, myelin basic protein; NeuN, neuronal nuclei; NSE, neuronal-specific enolase; GAD, glutamate decarboxylase; BSA, bovine serum albumin; GABA, 7-aminobutiric acid.

[2]References: 1, Wenthold RJ, Yokotani N, Doi K, Wada K. 1992. J Biol Chem 267:501-507. 2, Petralia RS, Wang Y-X, Mayat E, Wenthold RJ. 1997. J Comp Neurol 385:456-476. 3, Moga DE, Janssen WG, Vissavajjhala P, Czelusniak SM, Moran TM, Hof PR, Morrison JH. 2003. J Comp Neurol 462:15–28. 4, Osborn M, Debus E, Weber K. 1984. Eur J Cell Biol 34:137-143. 5, McLendon RE, Burger PC, Pegram CN, Eng LF, Bigner DD. 1986. J Neuropathol Exp Neurol 45:692–703. 6, Personal observation. 7, Sommer I, Schachner M. 1981. Dev Biol 83:311–327. 8, Bansal R, Warrington AE, Gard AL, Ranscht B, Pfeiffer SE. 1989. J Neurosci Res 24:548–557. 9, Dyer CA, Kendler A, Philibotte T, Gardiner P, Cruz J, Levy HL. 1996. J Neuropathol Exp Neurol 55:795–814. 10, Lind D, Franken S, Kappler J, Jankowski J, Schilling K. 2005. J Neurosci Res 79:295–302. 11, Chemicon International technical information. 12, Chang YC, Gottlieb DI. 1988. J Neurosci 8:2123–2130. 13, Sigma technical information.